IS-T-736

SYNTHESIS AND CHARACTERIZATION OF SOME REDUCED ZIRCONIUM HALIDES

Richard Lynn Daake

Ph. D. Thesis Submitted to Iowa State University

Ames Laboratory, ERDA
Iowa State University
Ames, Iowa 50011

Date Transmitted: February 1977

PREPARED FOR THE U.S. ENERGY RESEARCH AND DEVELOPMENT ADMINISTRATION UNDER CONTRACT NO. W-7405-eng-82

DISCLAIMER

Available from: National Technical Information Service
U. S. Department of Commerce
P.O. Box 1553
Springfield, VA 22161

Price: Microfiche $3.00

TABLE OF CONTENTS

Synthesis and characterization of some reduced zirconium halides*

Richard L. Daake

Under the supervision of John D. Corbett
From the Department of Chemistry
Iowa State University

High temperature equilibrium experiments have revealed several new zirconium subhalides as well as nonstoichiometry among the better-known trihalides. Product characterization by standard gravimetric and electron microprobe analyses was allied with X-ray powder and single crystal work. Accurate lattice parameters for phases of known cell type were determined from high precision X-ray powder data obtained by Guinier methods with Si powder as an internal standard. Weld-sealed Ta tubing served as a strong inert container material for all subhalide reactions.

Up to 50 g batches of ZrCl and the hitherto unreported ZrBr have been prepared stoichiometrically from ZrX_4 and thin (3-4 mils) Zr turnings. Virtually 100% yields of > 99.5% pure $ZrCl_3$ and $ZrBr_3$ were subsequently made by reacting well-ground mixtures of ZrX_4 with the very soft graphitic monohalides. Since ZrI does not exist, ZrI_3 was prepared from ZrI_4 and $ZrI_{1.8}$, the most reduced iodide phase.

Lower and upper phase limits of the trihalides have been determined

---

*USERDA Report IS-T-736. This work was performed under Contract W-7405-eng-82 with the Energy Research and Development Administration.

from equilibrations of $ZrX_{3.0}$ with "ZrX_2" and ZrX_4, respectively. As expected, phase breadths increase from X=Cl to X=I. Lattice parameter shifts were measured as a function of composition for ZrX_3 (X=Br,I).

New compounds in the Zr-Cl and Zr-Br systems were prepared either by isopiestic equilibration of ZrX and ZrX_3 and/or via transport in a thermal gradient. One equilibrium subbromide phase, $ZrBr_{1.8}$, and two subchlorides, $ZrCl_{1.7}$ and $ZrCl_{2.5}$, have been identified, and powder patterns of $ZrBr_{1.8}$ and $ZrCl_{1.7}$ have been indexed on hexagonal unit cells.

A single crystal structure determination has shown the $ZrCl_{2.5}$ phase to be the first Group IVB M_6 cluster compound. It crystallizes in space group Ia3d with Z=16 and is isostructural with Ta_6Cl_{15}. The structure consists of $Zr_6Cl_{12}^{3+}$ units linked via intercluster bridging Cl atoms. The M_6 group is approximately octahedral with an average Zr-Zr distance of 3.207(4) Å. All clusters are symmetrically equivalent and each is bridge-bonded to only six of its eight near neighbors.

ZrBr has been shown from powder intensity data to be similar but not isostructural with ZrCl. Both have the $R\bar{3}m$ space group and show a 3-slab c axis repeat of pseudo cubic close packed (abca) X-M-M-X 4-layer sheets with strong interlayer Zr-Zr and Zr-X bonding but weak interslab (X-X) bonding. They differ only in the interslab stacking sequence, with coordination about halogen trigonal antiprismatic in ZrCl but prismatic in ZrBr. Valence region XPS spectra of both metallic phases show a d band extending to the Fermi level.

INTRODUCTION

Investigations of binary transition metal subhalides in recent years have revealed a large number of new compounds with an intriguing variety of structural and physical properties allied with a propensity toward metal-metal bonding. Since 1960 several reviews of the structural chemistry of metal-metal bonded transition metal halides have appeared in the literature (1-8).

The type of metallic aggregation in these compounds varies from simple pairing in α-NbI_4 (9) to extended two-dimensional double metal sheets in ZrCl (10,11). Between these extremes are found the M_3 units of Nb_3Cl_8 (12), $M_6X_8^{n+}$ and $M_6X_{12}^{n+}$ groups with various degrees of inter-cluster halogen bridge bonding which yield two-dimensional (e.g., Nb_6Cl_{14}) (13) or three-dimensional (e.g., Ta_6Cl_{15}) (14) network structures, the infinite metal chain structure of β-$ZrCl_3$ (15,16), and a number of potentially nonstoichiometric layered MX_2 polytypes.

The development of experimental methods for preparation of high purity transition metal subhalides has been the object of considerable research. A few reduced transition metal halides such as Re_3X_9 (X=Cl, Br,I) vaporize congruently and can therefore be purified simply by sublimation (17,18). However, this tendency markedly decreases as one moves to the left in the transition metal series, yielding to disproportionation to metal and higher volatile halides.

For the group IVB metals, a majority of the chemical literature of the halides has focused on the optimization of yield and purity of the

MX_3 phases and their disproportionation behavior. Heretofore, with the exception of ZrCl (10), compounds more reduced than the trihalides were either unknown or very poorly characterized. Most of the synthetic work on these systems has been in glass containers probably for lack of equipment to seal inert materials like Ta under vacuum or in an inert atmosphere.

Since the original preparation of $ZrCl_3$ in 1923 by Ruff and Wallstein (19) via reduction of $ZrCl_4$ with Al, numerous experimental approaches to the preparation of pure zirconium subhalides have appeared in the literature.

Newnham and Watts (20) obtained very finely divided superstoichiometric blue-black trihalides (X=Cl,Br,I) in small yields by atomic hydrogen reduction of $ZrX_4(g)$ in a glow discharge. Although not contaminated with metal or lower halides, the products gave unreportably poor X-ray powder diffraction patterns.

Watt and Baker (21) attempted preparation of ZrI_3 by reducing ZrI_4 with a variety of metals (Al,Fe,Ge,Hg) which form volatile iodides. Aluminum was concluded to be the best reductant tried, but it was still incompletely consumed after heating with a large excess of ZrI_4 at 300° for ten weeks.

Both Struss and Corbett (22) and Copley and Shelton (23) report easy product separation and good yields of green macrocrystalline trichloride by a non-equilibrium reduction of molten $ZrCl_4$ with an excess of Zr foil. After a 3-day reaction period at 410°, Copley and Shelton obtained 3-5g

yields of olive-green needles mixed with a small quantity of unreacted $ZrCl_4$ which was sublimed from the trichloride at 115°. The composition of their product varied between $ZrCl_{2.8}$ and $ZrCl_{3.0}$ depending on the extent of heat-treatment. Struss and Corbett (22) obtained somewhat larger yields by employing the more forcing conditions of a 12-day 600°/500° reaction in a weld-sealed tantalum container and, although analytical data were not given, their powder pattern was reportedly in excellent agreement with those of Dahl, et al., (15) and Watts (16) for $ZrCl_3$.

Troyanov, et al., (24) also achieved high yields of >99% pure $ZrCl_3$ by reduction of $ZrCl_4$(l) at 550° and 60 atm with Zr powder in a rotated autoclave which contained 1 cm steel balls for exposure of fresh metal surface. This technique was found superior to the stationary bomb method employed by Troyanov, Marek, and Tsirel'nikov (25) to prepare $ZrBr_3$ by heating metal powder with $ZrBr_4$(l) for 3-4 weeks at 480-500° (30-40 atm). Larsen and Leddy (26) who also used a stationary bomb technique found several cycles of regrinding followed by reheating at 500-700° necessary to obtain ZrX_3 (X=Cl,Br,I) of "reasonable" purity. (No detectable reduction of ZrF_4 was observed even after three days at 700°.) Dahl, et al., (15) also used this method to prepare ZrX_3 powders for structural studies and always found metal in the powder patterns of their products. The reported weight percentages of unreacted zirconium (38.8, 3.0, and 3.4 for X=Cl,Br, and I, respectively) were computed from analyses assuming admixture with $ZrX_{3.00}$ and absence of either intermediate phases or ZrX_3 nonstoichiometry.

Nonstoichiometry of the Zirconium Trihalides

Although the literature of the zirconium trihalides contains frequent reference to their nonstoichiometry, the nonequilibrium nature of many experiments which have been purported to yield nonstoichiometric trihalides and the lack of good X-ray data to demonstrate phase purity leave much to be desired.

Previous thermogravimetric effusion studies of ZrX_3 disproportionation at temperatures up to 450° suggest that the trichloride (23) and tribromide (27) are not line compounds but exist over a range of homogeneity from $ZrX_{2.8}$ to $ZrX_{3.0}$ with no detectable change in the powder pattern. (A shear mechanism has been proposed for the associated structural effects (23).) However, because of the nonequilibrium nature of the disproportionation method, and the very poor crystallinity of the "second stage" $ZrCl_{1.6}$ and $ZrBr_{1.1\text{-}1.4}$ residues claimed to form by further disproportionation, the "first stage" $ZrX_{2.8}$ residues may well contain undetected "second stage" products. Troyanov and Tsirel'nikov used similar methods to obtain "first stage" compositions of $ZrCl_{2.82}$ (28) and $ZrBr_{2.75}$ (25). However, their "second stage" products were claimed to be pure stoichiometric dihalides but again were poorly crystalline and characterized only by elemental analyses which offers no proof of phase purity.

The disproportionation behavior of ZrI_3 is also difficult to assess from the literature. Sale and Shelton (29) have suggested that $ZrI_{2.86}$ and $ZrI_{2.0}$ compositions prepared by triiodide disproportionation are

distinct phases and conclude that both are structurally similar to ZrI_3 because of the strong similarity of their powder patterns to that of the stoichiometric triiodide. However, admixture of amorphous lower iodides with undisproportionated triiodide may have led to incorrect conclusions from these nonequilibrium experiments. Baev and Shelton (30) have reported heats of formation for a number of ZrI_n "phases" (n=3.2, 3.17, 3.0, 2.8, and 2.5), but no X-ray or analytical data were given.

Perhaps the most conclusive evidence in the literature for nonstoichiometry of a zirconium trihalide is that presented by Troyanov, Marek, and Tsirel'nikov (25) who observed a steady decrease (with increasing composition) for the hexagonal $\underline{a}$ lattice parameter of $ZrBr_x$ prepared by annealing $ZrBr_{2.75}$ under $ZrBr_4(g)$ pressures of 4, 20, and 760 torr but at unspecified temperatures for unspecified durations. They reported that $\underline{a}$=6.738(2) Å for $ZrBr_{3.0}$ and 6.752 Å for $ZrBr_{2.8}$ based on diffractometer data but gave no indication of any corresponding change in the $\underline{c}$ parameter. Analogous "equilibrations" of $ZrCl_{2.8}$ (first stage $ZrCl_3$ disproportionation residues) with $ZrCl_4$ in sealed tubes at 320° (50 torr) and 370° (200 torr) for unreported durations produced final residues of $ZrCl_{2.80}$ and $ZrCl_{2.99}$, respectively, both of which gave the same hexagonal $\underline{a}$ parameter of 6.373(3) Å (28). (It is doubtful that equilibrium was even closely approached in the 320° experiment, but probably was at 370°.)

With the exception of products prepared by atomic hydrogen reduction (20) of $ZrX_4(g)$, the only hitherto reported superstoichiometric zirconium trihalide is the $ZrI_{3.2}$ composition made by Baev and Shelton via reduction of $ZrI_4(l)$ with an excess of Zr foil (30). However, in the absence of

X-ray powder data it is not clear that this product was a pure phase.

In related equilibrium work Struss and Corbett (31) have shown that hafnium triiodide has a compositional range of homogeneity at 475° ($3.0 < I/Hf < 3.5$) with a clear variation in both hexagonal lattice constants.

Single crystals of ZrX_3 have been grown by Larsen, et al., (32,33) from an Al_2X_6 - ZrX_4 eutectic melt by reduction of solvated Zr(IV) with Al chips or Zr powder at 230-310°; a single crystal structure of $ZrBr_3$ has recently been completed (34). Unfortunately MX_3 yields are relatively low, and slow contamination with a brown microcrystalline disproportionation product of approximate composition $(ZrX_2)_2\ AlX_3$ occurs in the chloride and bromide systems. The fact that the same decomposition products are obtained by digesting ZrX_3 in the corresponding molten aluminum trihalides suggests that the pure zirconium trihalides are not thermodynamically stable in the presence of excess Al_2X_6, thus eliminating this method for quantitative preparation of ultra pure trihalides. Reduction of a $ZrCl_4$-Al_2Cl_6 eutectic melt (76 mole percent Al_2Cl_6) at 200° with a deficiency of Zr metal has produced black hexagonal prisms of a novel ternary phase $Zr_{12}Al_4Cl_{52}$ (35) which has an average oxidation state of 3.33.

Lower Halides

Swaroop and Flengas (36) reported preparation of zirconium dichloride by reduction of $ZrCl_3$ with a 50% excess of Zr powder in a Pt-lined fused silica ampoule. However, their "$ZrCl_2$" powder pattern shows considerable

overlap with that of $ZrCl_3$ as well as other unidentified lines which do not correspond to any phases found in this laboratory.

Copley and Shelton (23) obtained constant-weight residues analyzing as $ZrCl_{1.6}$ from thermogravimetric effusion studies of the trichloride disproportionation over the temperature range 310-450°. Similar studies on $ZrBr_3$ (27) between 325° and 425° yielded $ZrBr_x$ residues of variable composition ($1.1 < x < 1.4$). Unfortunately, all of these "second stage" residues gave very diffuse X-ray diffraction patterns of unreportable quality.

ZrI_3 disproportionation at 360-390° in a glass tube with one end protruding from the furnace to permit condensation of ZrI_4 was reported by Sale and Shelton (37) to produce stoichiometric diiodide. However, the absence of reportable analytical data, the striking similarity of the reported X-ray powder data to that of ZrI_3, and the low reaction temperatures leave the suspicion that their product may well have been a mixture of triiodide with a more-reduced but amorphous material. Because of the nonequilibrium nature of the disproportionation experiment, and the possibility of reactions with glass, it is doubtful that any such residues represent pure phases.

A number of workers have inferred or assumed the presence of stoichiometric dihalides in thermodynamic studies of the $MX_3/"MX_2"$ equilibrium in the Zr-Cl (28,38,39), Zr-Br (25,40,41), and Zr-I (29) systems, and similarly in the Ti-Br (42) and Ti-I (43) systems. Atomic hydrogen reduction of finely-divided ZrF_4(s) at 350° has been purported to produce a black (metastable) "difluoride", but yields were extremely low (< 10 mg)

and analytical data of questionable accuracy (44). High temperature ($>700^{\circ}$) equilibrations of ZrF_4 with excess Zr foil in this laboratory have indicated that there are no reduced equilibrium phases in this system (45).

In static thermodynamic studies of the Zr-Cl system, Uchimura and Funaki (39) interpreted the four breaks they observed in the P versus T curve in terms of equilibria between compositionally adjacent pairs of the (assumed) stoichiometric "phases" $ZrCl_4$, $ZrCl_3$, $ZrCl_2$, ZrCl, and Zr. In spite of the poor agreement of their $ZrCl_3/ZrCl_2$ equilibrium measurements with those of other workers, their results on the $ZrCl_2/ZrCl$ ($560-680^{\circ}$) and ZrCl/Zr ($750-900^{\circ}$) equilibria are the only available data. The free energy of formation they report for ZrCl (56.1 kcal/mol) is probably more reliable than Dean's value of 68.4 kcal/mol determined electrochemically in aqueous HCl. (He originally prepared ZrCl (patent name "Zirklor") via reduction of a $SrCl_2$-NaCl-$ZrCl_4$ melt (63:34:3) onto graphite at 650° (46).)

Struss and Corbett (22) have reported preparation of highly crystalline stoichiometric ZrCl by an isothermal equilibration of $ZrCl_{1.4}$ (obtained from a preliminary reduction of $ZrCl_4$) with an excess of fresh metal foil in a sealed Ta container. Troyanov and Tsirel'nikov (47) employed a two-zone furnace to heat Zr foil at $750-800^{\circ}$ in a molybdenum glass boat at one end of a quartz ampoule while maintaining solid tetrachloride at its sublimation temperature of 330° (1 atm) at the other end. Black gleaming scales of ZrCl found growing on the foil gave an X-ray pattern virtually identical to that reported by Struss and Corbett (22)

except for nonobservance by Troyanov and Tsirel'nikov (47) of the line at d=9.73 Å. These workers also reported rhombohedral lattice parameters of $\underline{a}$=9.12(1) Å, α=21.62(8)°, space group $R\bar{3}m$, and a calculated density of 4.69g/cm^3 for Z=2.

That the structure finally published by Troyanov (48) was in serious error (R=0.29) has been amply discussed by Adolphson (10) who recently completed refinement of the ZrCl structure on a monclinic cell to a residual of 8%. The hexagonal platelet which he used for data collection was prepared in Ta by a 30-day reaction-equilibration of $ZrCl_4$ with a large excess of electropolished Zr foil in a 700°/900° temperature gradient. His single crystal dataset has since been re-refined on a hexagonal cell in space group $R\bar{3}m$ for an alternate structural perspective (11).

Essentially, the structure of ZrCl consists of close packed sheets of Zr or Cl atoms each with an intrasheet atom separation of 3.42 Å (the hexagonal $\underline{a}$ parameter) bound tightly via strong Zr-Zr and Zr-Cl intersheet interactions into Cl-Zr-Zr-Cl slabs in a pseudo cubic close packing (abca) arrangement. These slabs then stack along the $\underline{c}$ direction in the sequence abca bcab cabc (hereafter abbreviated A-B-C) to give a 3-slab repeat of 26.6 Å. (Refined lattice parameters based on Guinier powder data will be presented later in this work.) The long interlayer Cl-Cl distance of 3.61 Å is commensurate with a weak (van der Waals) interaction between slabs, which apparently gives rise to the graphitic nature of this material.

Purpose of the Present Work

Among the goals of the work reported here have been the development of simple techniques for improving product yield and purity of ZrX_3 (X=Cl, Br,I), the study of the nonstoichiometry of these phases, and determination of more precise lattice constants for them. However, the primary emphasis here has been the preparation and characterization of compounds more reduced than the trihalides in the Zr-X (X=Cl,Br,I) systems. Although compositions with $X/Zr < 3.0$ have been obtained by several workers using nonequilibrium methods, none of these residues have been properly characterized by X-ray diffraction, and reported elemental analyses are therefore of little value since phase purity was not established.

EXPERIMENTAL PROCEDURE

Preparation and Handling of Compounds

Preparative methods

Zirconium tetrahalides were prepared by reaction of halogen with a 10% excess of reactor-grade ($\sim$0.05% Hf) Zr foil at 400° followed by sublimation of the product back over the hot metal and through a coarse frit to remove entrapped halogen. Further purification was accomplished by vacuum sublimation at $<10^{-5}$ torr. Subsequent transfers and manipulations of these and all other zirconium compounds were carried out in a dry box with an atmosphere of pre-purified nitrogen which constantly recirculated through a column of Molecular Sieve.

Tantalum tubing with caps or crimps weld-sealed under 0.5-1 atm He served as a strong inert container for preparation of all reduced compounds. For large batches of ZrX, 10-25 cm long, 13 or 19 mm o.d. tubes with 0.4 mm walls were fitted with 0.7 mm thick formed Ta caps to provide the durability necessary to withstand intermediate reaction pressures of 20-40 atm.

With the advantage of Ta containers, the preparation of decagram quantities of high purity ZrX and ZrX_3 (X=Cl,Br) is quite facile. However, obtaining pure intermediate phases requires more sophistocated techniques and often much longer reaction times. Even then, only milligram yields of some phases are obtained via transport in a temperature gradient.

Biphasic isothermal equilibrations of nonadjacent phases (e.g., ZrX

and ZrX_3) have been done in tubes of various design. The simplest experiment involves placing reacting materials in opposite ends of a short, sealed tube partially crimped in the middle. A more suitable design employs concentric 9.5 and 6.4 mm o.d. tubes crimp-welded together at one end with the outer tube capped at the other. Reaction containers of this type can withstand internal pressures up to 30 atm but were rarely used under such stringent conditions. In cases where the total equilibrium pressure of reactive gas phase species (mostly ZrX_4) was expected to be considerably less than that of the He present, and especially when an intercompartment constriction served to separate solid phases, the Ta caps were electron-beam welded under vacuum.

A third type of biphasic equilibration was designed to estimate the equilibrium $ZrX_4(g)$ pressure in a two-phase region by a restricted volume decomposition of a pure phase. The starting material filled a 1-2 cm long, 6 mm o.d. crimped but unwelded tube which was contained in a larger sealed tube of known volume. The system was slowly heated to a desired equilibration temperature for a few days, and quenched whereupon $ZrX_4(g)$ condensed onto the walls of the outer tube but did not rereact appreciably with the solid phase because of the crimp in the smaller tube. The equilibrium $ZrX_4(g)$ pressure ($\pm$ 10%) was then calculated based on analysis of ZrX_4 for halogen and on the free volume.

The method of Struss and Corbett (22) was employed for preliminary preparation of ZrCl and ZrBr. While the use of Zr foil does permit clean product separation from the metal, the strongly-adhering nature of this product required considerable laborious scraping. Furthermore, first

batch yields had compositions of $1.3 < X/M < 1.5$ which necessitated reequilibration with a large excess of clean foil to obtain a layer of the pure monohalide. The development of a fairly thick product layer (2-4 mils) on the foil suggested the possibility of complete consumption of the metal if sufficiently thin Zr turnings were employed.

High purity (>99.5%) ZrCl and ZrBr were prepared stoichiometrically in decagram quantities and virtually 100% yields from 3-4 mil Zr turnings and ZrX_4. A one week reaction period at 450° served to reduce most of the ZrX_4 to ZrX_3 and was followed by a slow elevation of the temperature over the next 5-8 days to 825° where it was maintained for another week before air cooling.

This technique has not only improved reaction efficiency by permitting complete consumption of the Zr, but has made possible the quantitative preparation of up to 50 gram batches of high purity ZrCl and ZrBr which show no metal lines in the X-ray powder patterns.

In practice, compositions of $1.01 < X/M < 1.03$ are prepared to ensure that all metal is consumed. The product is ground, then screened through a 100 mesh sieve as a final precaution to remove any product chunks which may result from the presence of a few unusually thick turnings. (Less than 0.1% by weight of a typical product fails to pass this test.)

The availability of pure ZrCl and ZrBr has in turn simplified production of sizable quantities of >99.5% pure $ZrCl_3$ and $ZrBr_3$ by heating stoichiometric amounts of ZrX and ZrX_4 to 500° for a few days followed by cooling to 150° over a 2-3 day period before quenching. This procedure is

particularly fruitful because the relatively hard ZrX_4 acts as a grinding agent for the very soft, graphitic monohalides to produce a large ZrX surface area and thereby greatly reducing kinetic problems which have plagued reduction of the tetrahalides by Zr powder. Because of the non-existence of ZrI, the triiodide is prepared from ZrI_4 and the diiodide.

Although glass may be a suitable container for preparation of the trihalides by heating well-ground stoichiometric mixtures of ZrX and ZrX_4 at 400-500°, it is probably not sufficiently inert to be acceptable for reactions or equilibrations at much above 600°.

Product Characterization

Analytical procedures

Elemental analyses for Cl or Br were done by dissolving 0.2-0.4 g subhalide samples in approximately 10 ml of a solution 1.5 M each in HF and HNO_3 using a capped polyethylene bottle to prevent loss of HX during the exothermic dissolution. Subiodide samples were placed in ground-glass stoppered flasks containing 25 ml of a solution 0.5 M each in HF and HNO_3 and 0.1 g dissolved hydrazine sulfate to reduce the I_3^- formed initially to I^-. (In 1 M acid, several hours are required to yield a colorless solution.) Halogen analyses were completed by standard gravimetric techniques.

Analyses for Zr were performed by weighing 0.3-0.6 g samples by difference directly into a preweighed crucible, which was then placed into a mortar containing a few ml of water, covered with a watch glass, and

heated in an oven at 120° for a few hours. Reaction of the sample with water vapor leaves a white residue which is then fired to the oxide.

The electron microprobe was used to estimate X/M ratios for transported phases as these were never available in >100 mg quantities.

X-ray diffraction techniques

Debye-Scherrer powder patterns for qualitative work were taken on a 11.46 cm camera using Ni-filtered Cu K_α radiation. Powder patterns of excellent quality for high precision line position measurements (±0.02 mm, ±0.005°) were obtained with the evacuable Model XDC-700 Guinier camera (IRDAB, Stockholm) equipped with a quartz monochromator to provide a clean Cu K_{α_1} incident beam. A high precision millimeter scale was photographically printed on the front side of the film using an IRDAB Model XDC-750 scaling device. This procedure eliminates the need for a film shrinkage correction. The back side of the film was covered with a paper tape before developing to maximize line and scale sharpness and to minimize parallax in reading the film.

Special techniques were developed for preparation and transfer of air sensitive samples for Guinier patterns. A small amount (~0.1 mg) of a 200 mesh Si powder (NBS standard reference material 640) was mixed with ~0.5 mg of sample and tamped firmly onto the center portion of a 7 mm diameter circle of Scotch tape mounted over a 5 mm hole in a polyethylene holder. The small circular piece of tape containing the sample was in turn placed on the adhesive side of a larger piece of tape by which it was fastened to one side of a circular brass sample holder before transfer to

the camera in a small metal can.

In cases where multiple photographs of different duration were desired for the same sample, the camera box was backfilled with air just long enough (<5 sec) to remove the film cassette and then reevacuated during film development and reloading. Even for the extremely air and moisture sensitive trihalides, line broadening was never noticed for successive films nor for $ZrCl_3$ or $ZrBr_3$ samples stored for several days in the dry box or in evacuable containers. However, the triiodide does appear to react slowly with the Scotch tape. Therefore, Guinier patterns of ZrI_3 were taken immediately after loading the sample.

One of the major drawbacks of the flat-plate Guinier technique is the tendency of morphologically anisotropic crystalline substances to take on a preferred orientation, resulting in enhancement or attenuation of certain reflections. Although this effect reduces the reliability of Guinier intensity data (particularly for platelet phases), it is sometimes possible to use this effect to learn something about the orientation of the unit cell with respect to crystal morphology or perhaps to gain valuable insight into interreflection relationships which can in turn aid in indexing the powder pattern of a particular phase.

Since preferred orientation does not affect line positions, the Guinier technique can be used to obtain very precise lattice constants for phases of known cell type. Raw film scale readings for both Si standard and sample lines were input to the Guinier Film Measuring Program (GFMP) written by Robert L. Daake. This program computes an extrapolated index ($\theta=0^\circ$) based on each input Si line, a camera constant, and produces

standardized values of θ, d, $10^4 d^{-2}$, and $10^4 \sin^2\theta$ for each sample line.

When refined cell constants are to be computed for indexed phases, values of hkl and 2θ for a number of unambiguously assignable reflections are input to the Cell Dimension Refinement (CDR) program written locally by F. Takusagawa. The constants so obtained are then input to the 1969 version of the Parthé program (49) to obtain calculated line positions for comparison with the observed powder pattern. This program has also been used to compute line intensities corrected for Lorentz-polarization according to the reflection geometry and method of monochromatization of the incoming X-ray beam.

XPS studies

X-ray photoelectron spectra of Zr, ZrCl, ZrBr, and $ZrCl_4$ were taken by Dr. Mirtha Umaña at Argonne National Laboratory on a McPherson ESCA 36 photoelectron spectrometer with a Mg K_α source and modified for handling air and moisture-sensitive compounds by marriage with an argon atmosphere dry box (2-6 ppm H_2O and O_2) attached to the spectrometer via an O-ring flange.

Measurements were made under a vacuum of $<10^{-9}$ torr with a several atom layer of gold vaporized onto potentially insulating samples for calibration. Ten-scan spectra of desired regions were taken over 20eV intervals of 111 points each.

Single crystal work

Although oscillation photographs of single-appearing ZrX_x crystal platelets of uncertain composition ($1.6 < x < 1.8$ for X=Cl; $1.8 < x < 2.0$ for X=I) give single spots, zero and first level photographs of both phases show extensive streaking along the translation axis indicating their unsuitability for single crystal structure determinations. Approximate lattice parameters were obtained from these films, however.

A very small (0.03 mm diameter) and nearly spherical gem-like crystal of a hitherto unreported phase in the Zr-Cl system was found acceptable for the collection of three-dimensional single crystal data on an automated (50) four-circle diffractometer with Mo K_α radiation ($\lambda = 0.70954$ Å).

Crystal alignment was accomplished by inputting to the computer 12-17 operator-measured polar coordinates for spots on Polaroid films taken at several arbitrary crystal orientations. These reflections were searched and tuned by the instrument to obtain precise values of χ, ϕ, ω, and 2θ. The computer then assigned best-fit small integral indices to these reflections and output lattice parameters, cell scalers, an orientation matrix for the selected unit cell, and indices of the input reflections. At this point a rhombohedral to cubic cell transformation option was evoked after which three noncoplanar moderately strong reflections of fairly high 2θ were selected as standards for initial and periodic retuning during data collection ($0^\circ < 2\theta < 50^\circ$).

After checking the first 759 reflections for a primitive cubic cell, a body-centering extinction was indicated; reflections with h+k+l

(permutable) $\neq 2n$ were thereafter not checked. Of the 4267 allowed reflections, 1809 were observed with FOBS > 3SIGF and INT > 3SIGI. The systematic absence of hhl reflections for $2h + l \neq 4n$ eliminated eight of the ten body-centered space groups (51) while additional absence of 0kl reflections for k,(l) $\neq 2n$ prompted choice of the centric space group Ia3d (No. 230) as opposed to the acentric $I\bar{4}3d$ (No. 220). Removal of five symmetry extinct reflections (each "observed" only once and all among the six weakest reflections in the dataset) and elimination of 17 symmetry allowed reflections having $(|F_{obs} - F_{aver}| / F_{aver}) > 0.15$ left 1788 pieces of data which were averaged to give a final reduced dataset of 404 independent reflections.

The final lattice parameter refinement which gave $\underline{a}$=21.141(3) for the cubic cell was carried out by inputting the hkl and 2θ values of 14 moderately strong reflections to the CDR program.

RESULTS AND DISCUSSION

The Zirconium Trihalides

The present studies on the zirconium trihalides differ in a number of respects from those of other workers. First, the syntheses reported here involve isothermal equilibrations, not nonequilibrium disproportionations. Second, sealed Ta containers have provided both the inertness and strength which glass containers cannot provide at elevated temperatures and pressures, especially for prolonged periods. Third, higher reaction temperatures and considerably longer reaction periods have not only increased confidence in the attainment of equilibrium, but have also resulted in highly crystalline products for X-ray characterization.

Experimental evidence for nonstoichiometry

The compositions reported as phase limits in Table 1 were prepared in two-compartment Ta tubes by moderately long-term (6-22 days) equilibrations of trihalide with bracketing phases (e.g., ZrX_4 or "ZrX_2").

Indirect evidence that the triiodide phase may extend to a lower composition limit near $ZrI_{2.6}$ was obtained from an attempted stoichiometric preparation of ZrI_2 from ZrI_4 and Zr turnings. Since appreciable metal remained after eleven days at 750°, the product mixture was ground to expose fresh metal surface and reheated at 850° for five days, after which 40% of the metal was still unconsumed. In contrast to the strongly-adhering nature of ZrX (X=Cl,Br) on excess Zr foil or turnings, the ZrI_x product of this reaction was easily separated from the turnings by light grinding

Table 1. Nonstoichiometry of the zirconiun trihalides

Phase[a] Limit	No. Expts.	Product Color	Equilibrated With	Temp. (deg.)	Time (days)	P (atm.)	Analytical % Recovery
$ZrCl_{2.94}$[b]	2	olive-green	$ZrCl_{1.8}$	500	22	2	100.2
$ZrCl_{3.03}$	2	olive-green	$ZrCl_4$	440	9	20	100.1
$ZrBr_{2.87}$	1	olive-green	$ZrBr_{1.3}$	435	14	10^{-2}	Br only
$ZrBr_{3.23}$	2	blue-black	$ZrBr_4$	435	6	12	Br only
$ZrI_{<2.90}$[c]	1	blue-black	ZrI_2	-	-	-	I only
$ZrI_{3.40(5)}$[d]	1	green-black	ZrI_4	475	8	3	mass gain

[a]All products pure to X-rays.

[b]Two similar 7-day equilibrations at 600° (P > 25 atm) with a $ZrCl_3/ZrCl_2$ mixture gave products of compositions 2.87 (99.97% recovery) and 2.91 (100.00% recovery) which show small and trace amounts of $ZrCl_2$, respectively, implying that the trichloride lower limit is virtually temperature independent up to 600°.

[c]See text for discussion.

[d]Product stoichiometry was computed from mass gain assuming reaction with $ZrI_4(g)$.

followed by screening. A final product composition of $ZrI_{2.5}$ was estimated from the mass lost by the turnings.

Except for three weak lines of the diiodide (to be discussed in the next section), a Debye-Scherrer pattern of this $ZrI_{2.5}$ product was indexable on a β-ZrI_3 type hexagonal cell with $\underline{a}$=7.27 Å and $\underline{c}$=6.64 Å. This pattern is given in Table 2 along with the practically identical powder pattern reported by Sale and Shelton (37) for the "ZrI_2" residue of a ZrI_3 disproportionation. These workers noted a striking similarity between the powder pattern of their "diiodide" and that of the ZrI_3 starting material quite probably because their "diiodide" composition was actually a mixture of ZrI_3 (i.e., the triiodide lower limit) with more-reduced but amorphous products.

Although not an equilibrium product, $ZrI_{2.90}$ is also included in Table 1 because of the implication of substoichiometry. Approximately 1.5 g of this material was obtained as 5-15 mm long blue-black needles along with 0.2-0.3 g ZrI_4 and a few mg of I_2 (readily soluble in CCl_4) after an attempt to reduce a $ZrI_{2.5}$ composition at 900° for seven days in the presence of a large excess of Zr foil. The system pressure was estimated from the bulge in the Ta caps to be 15-20 atm (considerably higher than expected), with Zr apparently the only condensed phase at 900°. The $ZrI_{2.9}$ needles appear to have formed at a "cold" spot in the tube during slow cooling of the system in a Marshall furnace. The composition of $ZrI_{2.90}$ was determined by a standard gravimetric iodide analysis of 0.2 g of medium to large hand-picked needles.

Precise lattice parameter measurements of trihalides at various

Table 2. Comparison of a Debye-Scherrer pattern of a $ZrI_{2.5}$ composition with the literature pattern of zirconium "diiodide"

$ZrI_{2.5}$ (this work)[a]			"ZrI_2" (Sale and Shelton)[b]	
d_{obs}	I_{obs}	h k l	d_{obs}	I_{obs}
7.35*	vw	-	-	-
-	-	?	7.091	vw
6.21	w	1 0 0	6.212	w
3.69*	vw	-	-	-
3.61	w	1 1 0	3.646	w
3.305	w	0 0 2	3.319	w
3.18	s	1 1 1	3.172	vs
-	-	1 0 2	2.945	vw
-	-	?	2.824	vw
-	-	?	2.695	vw
2.45	m	1 1 2	2.453	m
2.38	w	2 1 0	2.385	vw
2.31	vw	2 0 2	2.287	vw
2.097	s	3 0 0	2.097	vs
1.935	w	2 1 2	1.934	vw
1.890	w	1 1 3	1.891	m
1.855*	vw	-	-	-
1.780	w	3 0 2	1.776	w
1.753	m	2 2 1	1.753	m
1.660	vw	0 0 4	1.660	vw
1.595	mw	2 2 2	1.595	m
1.410	w	2 2 3	1.407	w
1.347	ms	4 1 1	1.347	s
1.305	w	3 0 4	1.304	m
1.272	w	4 1 2	1.270	m
1.250	vw	1 1 5	1.250	w
1.214	w	3 3 0	1.213	m

[a]Except for three (*) $ZrI_{1.8}$ lines, the pattern of $ZrI_{2.5}$ fits a β-ZrI_3 type hexagonal cell with $\underline{a}$=7.27Å and $\underline{c}$=6.64Å. (A Guinier pattern of $ZrI_{1.8}$ appears in Table A-1.)

[b]Reference 37.

compositions lend further support to nonstoichiometry for $ZrBr_3$ and ZrI_3. These results are presented in Table 3 along with comparative data for HfI_3. The hexagonal lattice parameters for $ZrBr_3$ at four different compositions are also plotted in Figure 1 as a function of composition.

Although the behavior of the ZrI_3 parameters parallels that of HfI_3 (a increases and c decreases as I/M increases), both parameters of $ZrBr_3$ decrease with increasing composition and with no apparent break at $ZrBr_{3.00}$ or superstructure lines in the powder patterns of nonstoichiometric compositions. For $ZrCl_3$, the composition range is fairly small ($2.94 < X/M < 3.03$) and no line position shifts have ever been observed in Guinier patterns of this phase.

The β-ZrX_3 (X=Cl,Br,I) structure was first deduced from powder data to consist of parallel linear chains of face-sharing ZrX_6 octahedra formed by filling appropriate octahedral holes in a close packed halide lattice (15,16). The tendency of macroscopic ZrX_3 needles (prepared in this laboratory) to fray into a multitude of very thin fibers when cut or crushed is a clear indication of the weak interchain bonding.

Magnetic studies on β-$TiCl_3$ (52) and β-MI_3 (M=Zr,Hf) (53), on the other hand, are consistent with strong intrachain metal-metal interactions, but whether the metal ions are paired or equally spaced along the chains was answered only recently. In a single crystal structure of $ZrBr_3$, Kleppinger, Calabrese, and Larsen inferred equal spacing from the near sphericity of the thermal elipsoids (34). It is puzzling, however, that the hexagonal lattice parameters, a=6.7275(20) Å and c=6.2992(14) Å, reported by these workers are nearly identical to those given here for

Table 3. Hexagonal lattice constants for nonstoichiometric zirconium trihalides[a] and hafnium triiodide[b]

Phase Composition	N[c]	a (Å)	c (Å)	Preparative Method
$ZrCl_{3.00}$	21	6.3842(4)	6.1341(5)	$ZrCl + ZrCl_4$ (450°,10d)
$ZrBr_{2.87}$	21	6.7565(5)	6.3245(5)	$ZrBr_3$--$ZrBr_{1.3}$ (435°,14d)[d]
$ZrBr_{3.00}$	21	6.7472(6)	6.3135(5)	$ZrBr + ZrBr_4$ (450°,14d)
$ZrBr_{3.10}$	21	6.7399(5)	6.3050(5)	$ZrBr_{3.00} + ZrBr_{3.23}$ (400°,7d)
$ZrBr_{3.23}$	21	6.7309(5)	6.2995(6)	$ZrBr_3$--$ZrBr_4$ (435°,14d)[d]
$ZrI_{3.0}$	26	7.285(1)	6.659(1)	$ZrI_{1.8} + ZrI_4$ (600°,10d)
$ZrI_{3.4}$	22	7.235(1)	6.698(2)	$ZrI_{2.9}$ -- ZrI_4 (475°,8d)[d]
$HfI_{3.0}$[b]	-	7.27(1)	6.58(1)	$HfI_{3.2}$ -- Hf (575°)[d]
$HfI_{3.5}$[b]	-	7.23(1)	6.67(1)	$HfI_{3.2}$ -- HfI_4 (475°)[d]

[a]This work.

[b]Reference 31.

[c]The number of unambiguously assigned lines input to the CDR program.

[d]Biphasic equilibration.

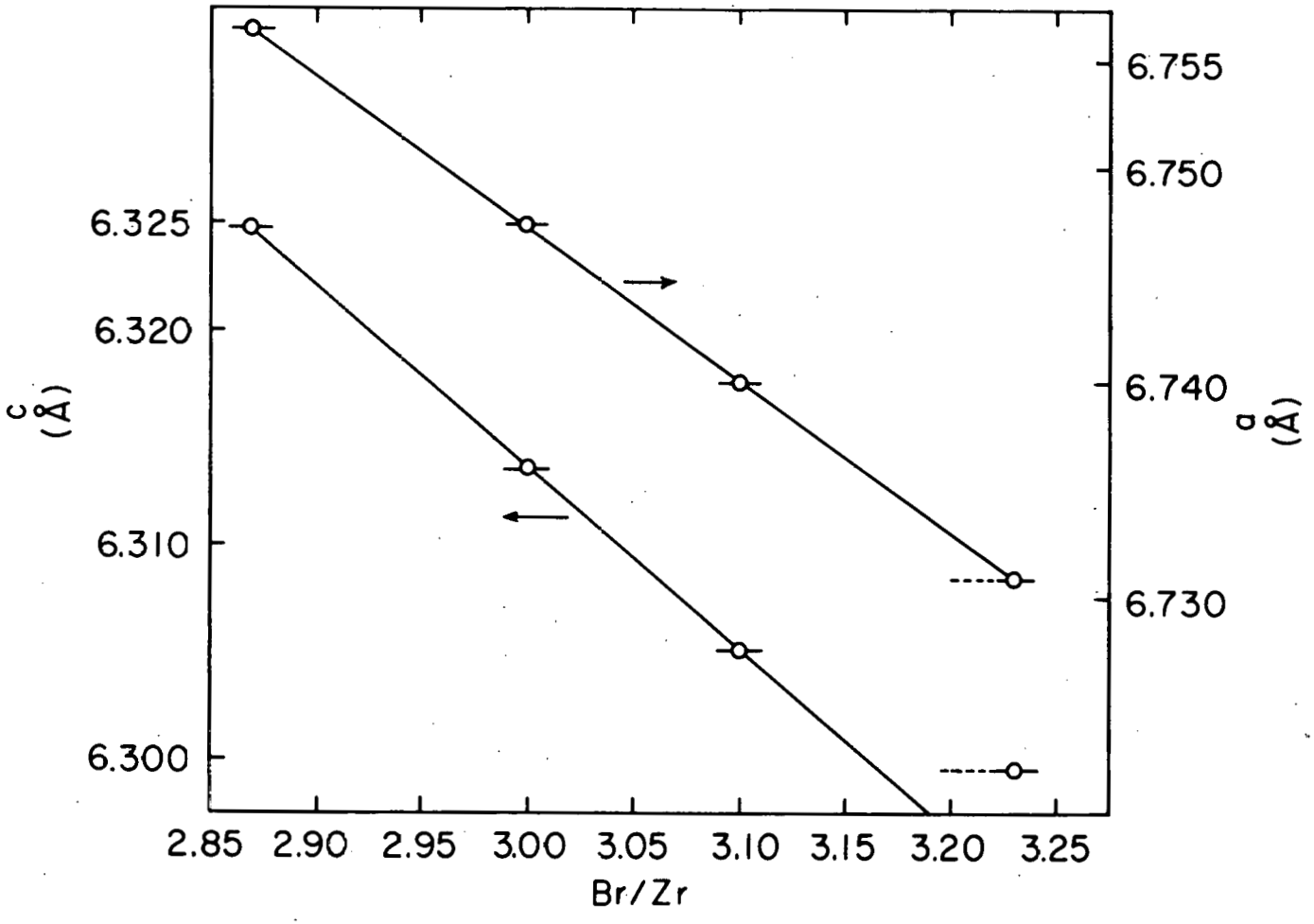

Figure 1. Variation of hexagcnal lattice parameters of β-$ZrBr_3$ with composition

$ZrBr_{3.23}$. Since the difference between a and c (Figure 1) remains fairly constant as the tribromide composition varies, it is not clear whether the independently determined lattice constants are accidentally similar because of different methods and/or standards for lattice constant determination, or whether the crystal used for data collection was unknowingly superstoichiometric.

A couple of observations support the latter postulate. First, the method of preparation described by Larsen, Moyer, Gil-Arnao, and Camp (32,33) involves reduction of a $ZrBr_4$-Al_2Br_6 eutectic melt with metallic Zr or Al at 270-290°. Brown-black hexagonal needles of $ZrBr_3$ reportedly grow separate from the metal near the gas-liquid interface by decomposition of some Zr(III)-containing solvated species. First batch yields are typically only 5%, and in light of the several mole ratio excess of solvated Zr(IV), it would be rather surprising for trihalide crystals grown under such oxidizing conditions not to approach the upper limit composition.

Secondly, single crystal needles of ZrX_3 grown by the above method are reportedly yellow-green for X=Cl, brown-black for X=Br, and black for X=I. In contrast, needles of slightly substoichiometric trihalides grown from the gas phase in this laboratory are golden-green for X=Cl,Br and blue-black for X=I while powders of stoichiometric ZrX_3 prepared here are olive-green for X=Cl,Br and greenish-black for X=I. Furthermore, $ZrBr_{3.23}$ prepared here by equilibrating olive-green $ZrBr_3$ powder with $ZrBr_4$ at 435° for 14 days is blue-black in color and leaves a deep blue halo on a mortar after grinding, while $ZrBr_{3.0}$ leaves a residual golden-green color.

Hence both color and conditions suggest that the recently reported

structure of β-$ZrBr_3$ was perhaps unknowingly done on a significantly superstoichiometric tribromide crystal. It is of particular interest that no superstructure was reported even though the examined crystal was grown at temperatures below 300° where long-range ordering of defects would be favored.

Mechanisms for nonstoichiometry

A shear mechanism for development of substoichiometry during ZrX_3 disproportionation has been proposed by Copley and Shelton (23), whereas a combination cation vacancy-substitution mechanism has been suggested by Struss and Corbett (31) for superstoichiometry in hafnium triiodide. The absence of an observable break at Br/Zr=3.0 in Figure 1 is rather puzzling in light of the difference in the mechanisms proposed for substoichiometry and superstoichiometry. Perhaps both mechanisms are operative in the neighborhood of $ZrBr_{3.00}$. However, a break in one or both lattice parameter curves does apparently occur somewhere between $ZrBr_{3.10}$ and $ZrBr_{3.23}$. The unsymmetrical dashed error bars in Figure 1 for the $ZrBr_{3.23}$ composition simply indicate the possibility of undetected $ZrBr_4$ which may have condensed onto the $ZrBr_{3+}$ upon cooling the high activity (P=12 atm) $ZrBr_4/ZrBr_{3+}$ system from 435°. It is certainly reasonable under these circumstances, although not provable from available data, that both curves might break simultaneously but in opposite directions somewhere between $ZrBr_{1.10}$ and $ZrBr_{3.23}$.

If, on the other hand, $ZrBr_{3.23}$ is a precisely pure phase, perhaps a break in only the c parameter can be understood in terms of a mechanism similar in principle but opposite in effect to the shear process proposed

by Copley and Shelton (23) for achieving substoichiometry in the β-ZrX_3 structure.

Charge balance requires satisfaction of the cation vacancy - substitution formalism proposed by Struss and Corbett ($4M_M^{3+}=3M_M^{4+}+V_M$) for HfI_3 superstoichiometry (31). The presence of extended Zr-Zr interactions along the metal chain in these structures eliminates the distinction between intrachain M^{3+} and M^{4+} ions. Occasionally isolated M^{4+} ions may occur in the otherwise empty interchain interstices, shortening the average chain length and decreasing the average interchain distance (the a lattice parameter).

The mechanism for substoichiometry proposed by Copley and Shelton (23) involves organization of additional metal atoms into 001 shear planes. Superstoichiometry on the other hand might give rise to 001 vacancy shear planes resulting in an increased repulsion along the c direction between adjacent halide layers which are bisected by these metal-vacancy planes. Although speculative, these ideas are consistent with a gradual decrease in the a parameter while allowing for a rather sudden attenuation of the decrease in the c parameter as the tribromide upper limit is approached.

The Zirconium "Dihalides"

In spite of relatively frequent reference to "dihalides" in the thermodynamics literature of the Zr-X systems, compositional and structural characterization of these materials has remained far from adequate.

The diiodide

The incomplete consumption of zirconium turnings in an attempted stoichiometric preparation of ZrI_2 by reaction with ZrI_4 at 750° for eleven days and 850° for five days is especially puzzling in light of the ease of making ZrCl and ZrBr by this method. From the shiny surface of the unconsumed (40%) metal, it at first appeared that ZrI_3 was the most reduced phase in the Zr-I system. However, the fact that further reduction was finally achieved by using fresh metal indicated that the surface of the turnings had become blocked with a thin product or impurity layer through which diffusion, and hence further reduction, became extremely slow. Reequilibration of the $ZrI_{2.5}$ with a 50-fold excess of fresh Zr foil at 750° for two weeks gave a loosely-adhering black platelet phase of composition $ZrI_{1.81}$ (99.93% recovery) on the foil. This material has a unique powder pattern (Appendix Table A-1) quite distinct from $ZrI_{2.5}$ and Shelton's "diiodide" (Table 2). Several other pure ZrI_x products made by reduction of ZrI_3 or ZrI_4 with a large excess of Zr foil or turnings invariably have compositions of $1.8 < x < 1.95$ with excellent (>99.8%) analytical recoveries and the same powder pattern. This phase will henceforth be referred to generically as the diiodide.

The morphology of the diiodide has been observed to vary from large

1-2 mm triangular or hexagonal platelets to needles up to 1 cm long. Close examination of these needles under the microscope revealed them to be stacks of paper-thin platelets randomly joined at various points. Their general overall appearance raised suspicion that they may have formed directly from ZrI_3 single crystals produced during an intermediate stage of the reduction.

In order to test the implied topotactic relationship between the ZrI_3 and ZrI_2 phases, a few well-formed needles of $ZrI_{2.90}$ (referred to in the previous section of this chapter) were heated very slowly to 750° over three days in the presence of excess Zr and maintained there for 15 days. Interestingly, the general crystal size and shape as well as the mirror-smooth platelet faces were retained, although the larger ZrI_3 single crystals had degenerated to needle-platelet bundles. Oscillation ($\pm 10°$) photographs of these crystals gave single spots when orientated with the platelet face perpendicular to the beam, but gave stacked multiple spots when the incident beam was roughly parallel to the platelet. However, in all cases the needle axis (also the spindle axis) gave a crystallographic repeat of 3.75 Å compared with a needle axis repeat of 6.70 Å for the triiodide single crystals from which they were derived.

One of the very small $ZrI_{1.8}$ crystals which gave no multiple spots was selected for zero and first-level Weissenberg photographs. In spite of very bad streaking of the spots along the translation axis (indicative of two dimensional disorder perpendicular to the spindle axis), the films were of sufficient quality to obtain approximate orthorhombic lattice parameters of $\underline{a}$=3.75 Å, $\underline{b}$=6.85 Å, and $\underline{c}$=15.0 Å.

The dibromide and sesquibromide

A number of static thermodynamic studies (25,40,41) have either produced or assumed $ZrBr_2$ compositions by thermal decomposition of $ZrBr_3$; vacuum disproportionation in an effusion cell (27) has yielded $ZrBr_x$ residues with x=1.1-1.4. Perhaps because of their poor crystallinity no X-ray powder data on any of these residues have been published. Hence the literature contains no conclusive evidence for, or X-ray characterization of, either a dibromide or any zirconium subbromide other than $ZrBr_3$.

In the present study, biphasic equilibrations of ZrBr with $ZrBr_3$ were employed as a major means of examining the intermediate region. However, because of the approximately stoichiometric "dibromide" residues claimed by some workers to form during tribromide disproportionation, preparation of a $ZrBr_{2.0}$ composition was attempted in this laboratory by heating a well-ground mixture of ZrBr and $ZrBr_4$ over seven days to 650° and equilibrating there for two more days. The olive-green product of this reaction was shown quite clearly from a powder pattern to consist of a mixture of $ZrBr_3$ and ZrBr with some new phase(s). The tribromide in this nonequilibrium multiphasic mixture was simply an outer layer on the product granules and was easily removed by washing with anhydrous acetone or 10% methanol in trichloroethylene. The excellent quality Guinier powder pattern obtained for the vacuum-dried black $ZrBr_x$ residue (x=1.32 based on Br) is given in Appendix Table A-2. The presence of perhaps 20-40% ZrBr in this material makes an estimated composition of $ZrBr_{1.5(1)}$ reasonable for this phase. Lines of the sesquibromide have appeared in powder patterns of numerous reaction products but always in the presence

of both ZrBr and $ZrBr_3$. They are especially prominent in reactions of relatively short duration and net compositions greater than $ZrBr_{1.5}$.

Longer duration preparations of compositions more reduced than $ZrBr_{1.7}$ produce a silvery-gray $ZrBr_y$ phase which has a much simpler powder pattern than that of the sesquibromide. Unfortunately, like the sesquibromide, this phase has never been obtained in pure form, but always as a coating on the ZrBr starting material and often in the presence of tribromide when net system compositions were more oxidized than $ZrBr_{1.3}$.

Apparently, attainment of thermodynamic equilibrium between ZrBr or $ZrBr_3$ and $ZrBr_y$, at temperatures where system pressures are manageable in Ta containers, may require many months. Experience has shown that both ZrBr and $ZrBr_3$ are much easier to prepare in pure form than are the intermediate phases. For example, a ZrBr-$ZrBr_4$ mixture (net reaction composition Br/Zr=1.7) was slowly heated over a 7-day period in a short tube of minimal free volume to 600° followed by a 26-day reaction period. The presence of an unintended temperature gradient resulted in product zoning--a hard olive-green plug of $ZrBr_3$ mixed with ZrBr and the new $ZrBr_y$ phase at one end, and a loose granular silvery-gray product containing $ZrBr_y$ and ZrBr but no tribromide and analyzing as $ZrBr_{1.42}$ (100.0% recovery) at the other end. A product of composition $ZrBr_{1.2}$ prepared under the same conditions is identical except for the relatively stronger ZrBr lines. Compositions $ZrBr_{1.15}$ and $ZrBr_{1.10}$ prepared by reacting ZrBr and $ZrBr_3$ for ten days at 750° also show corresponding new lines, but still more weakly. Judging from the intensity of $ZrBr_y$ lines relative

Table 4. Guinier powder pattern of $ZrBr_{1.42}$ ($ZrBr + ZrBr_{1.8(2)}$)

d_{obs}	I_{obs} $ZrBr_{1.42}$	$ZrBr_{1.8}$[a] h k l	ZrBr h k l	d_{obs}	I_{obs} $ZrBr_{1.42}$	$ZrBr_{1.8}$[a] h k l	ZrBr h k l
9.38	1		0 0 3	1.5267	3		1 1 9
6.88	4	0 0 2		1.5208	1		1 0 16
4.685	1		0 0 6	1.5157	1		2 0 1
3.434	1	0 0 4		1.5093	1		2 0 2
3.137	Si			1.4959	1	1 0 8	
3.055	5	1 0 0		1.4898	1	2 0 2	
3.019	2		1 0 1	1.4650	3		2 0 5
2.968	3		1 0 2	1.4481	4	2 0 3	
2.790	2	1 0 2	1 0 4	1.4197	1		2 0 7
2.671	7		1 0 5	1.4021	2		1 1 12
2.541	8	1 0 3		1.3964	2	1 1 6	
2.421	2		1 0 7	1.3573	Si		
2.338	1		0 0 12	1.3344	3	2 0 5	2 0 10
2.288	1	0 0 6		1.2787	1		1 1 15
2.280	1	1 0 4		1.2699	1	2 0 6	
2.061	2		1 0 10	1.2457	Si		
2.041	3	1 0 5		1.2295	2	1 1 8	
1.9203	Si			1.1541	2	2 1 0	
1.8307	1	1 0 6		1.1436	1	0 0 12	2 1 2
1.7633	10	1 1 0		1.1405	1	2 0 8	
1.7525	10		1 1 0	1.1380	1	2 1 2	
1.7224	1		1 1 3	1.1241	2		2 1 5
1.7159	1	0 0 8		1.1192	5	2 1 3	
1.7074	2	1 1 2		1.1158	1		2 0 17
1.6373	Si			1.1089	Si		
1.5676	1	1 1 4		1.1035	1		2 1 7

[a]The powder pattern of $ZrBr_{1.8(2)}$ is given in Appendix Table A-3 relative to a primitive hexagonal cell with a=3.5257(2) and c=13.726(2), and the Guinier pattern of ZrBr in Table A-6.

to those of ZrBr for various biphasic compositions, an extrapolated composition of $ZrBr_{1.8(2)}$ is reasonable for the pure new phase, hereafter referred to generically as the dibromide.

All 23 new lines in the powder pattern of $ZrBr_{1.42}$ (Table 4) have been indexed on a hexagonal unit cell with $\underline{a}$=3.5257(2) and $\underline{c}$=13.726(2) which is reasonable for, but does not prove, a 2-slab MX_2 type structure like those of 2S-$Nb_{1+x}Se_2$ (54,55).

The powder pattern of $ZrBr_{1.8}$ is given in Appendix Table A-3 in terms of the primitive hexagonal cell on which it has been indexed. Accidental overlap with three observed ZrBr lines is appropriately indicated and $ZrBr_{1.8}$ intensities for lines at those positions have been estimated by subtraction of overlapping intensities assuming a 50-50 mixture.

It can be inferred from the foregoing that the sesquibromide is probably a metastable phase prepared by rapid reaction of ZrBr with $ZrBr_4(g)$ under moderately oxidizing conditions and temperatures below 700°, while the substoichiometric "dibromide" may be the only thermodynamically stable phase between ZrBr and $ZrBr_3$. Unfortunately, serious kinetic problems have prevented preparation of this phase in high purity, hence determination of either phase limit has been thwarted.

The "dichloride"

X-ray diffraction data for a powdered product alleged to be zirconium dichloride was first published in 1965 by Swaroop and Flengas (36), but is in gross disagreement with results obtained in this laboratory. These workers reduced 95-99% pure $ZrCl_3$ with an excess of reactor-grade Zr

powder in a platinum-lined silica container. Analytical recoveries varied from 96% to 105%, and while the powder pattern of their product does not show lines of Pt or $PtCl_2$, the possibility of a ternary phase was ignored. This is particularly unfortunate in the light of a recent observation by Lascelles and Shelton (56) that ZrI_4 vapor reacts rapidly with both copper and silver even at 200° to give velvet-like MZr_3I_{12} products.

The only other powder diffraction data for "$ZrCl_2$" in the literature is that presented by Struss and Corbett (22) who first noticed transport of a Zr-rich phase while studying the reduction of MCl_4 with M(M=97% Hf, 3% Zr). Their preliminary powder pattern for the "dichloride" is substantially in agreement with that to be presented here.

Analogous to the Zr-Br system, an attempt to make stoichiometric $ZrCl_2$ (at 500°) from ZrCl and $ZrCl_4$ resulted in a three phase mixture of $ZrCl_3$, unreacted ZrCl, and a new phase with a very strong line at d=6.46 Å. An unintended temperature gradient had again resulted in product zoning into an olive-green plug at one end (containing 40-60% $ZrCl_3$), and a brownish-black free-flowing granular product at the other end analyzing as $ZrCl_{1.83}$ (based on two analyses for Zr) and which contained 5-10% unreacted ZrCl and 3-5% $ZrCl_3$. A two-compartment equilibration of this $ZrCl_{1.83}$ with ZrCl at 500° for 22 days gave a product ($ZrCl_{1.66}$, 99.97% recovery) with an identical powder pattern except for the complete absence of trichloride lines.

Another attempt was made to prepare an equilibrium $ZrCl_{2.0}$ composition from ZrCl and $ZrCl_4$ by the more forcing conditions of a 4-week reaction at 600° followed by grinding and reheating at 650° ($P \approx 40$ atm)

for two more weeks. Again, true thermodynamic equilibrium was not attained but was more closely approached since only a faint trace of ZrCl was evident in the powder pattern. However, sufficient $ZrCl_3$ (20-30%) was present to leave the impression that zirconium "dichloride" may well be substoichiometric even at its upper limit.

Approximately 20 g of a $ZrCl_{1.74}$ composition for use in biphasic equilibrations was prepared from ZrCl and $ZrCl_4$ via a 38-day reaction at 575°. A powder pattern of the homogeneous-looking granular blue-black product showed only a small amount of ZrCl (<10%) and a faint trace (1-3%) of $ZrCl_3$ which may have formed by reaction with $ZrCl_4(g)$ on cooling. Two-compartment equilibrations of the $ZrCl_{1.7}$ product with ZrCl at 605° for eleven days and at 700° for three days gave products of composition $ZrCl_{1.54}$ (99.98% recovery) and $ZrCl_{1.51}$ (100.12% recovery), respectively, indicating that the "dichloride" which coated unconsumed ZrCl crystallites in the $ZrCl_{1.7}$ mixture could indeed be further reduced by providing fresh (uncoated) ZrCl as a kinetically more accessible $ZrCl_4(g)$ sink.

The implication of a concentration gradient across the outer dichloride layer of $ZrCl_{1.7}$ product granules leads to inference of a homogeneity region for this phase. To test this postulate, biphasic equilibrations of a $ZrCl_{1.45}$ composition with dichloride/trichloride mixtures were performed for twelve days at 600° and fifteen days at 500°. Equilibrium was not even closely approached in the latter case, but at 600° a composition of $ZrCl_{1.75}$ (99.87% recovery) was obtained which showed a trace of $ZrCl_3$ and perhaps 5-8% ZrCl. With no knowledge of the composition profile

across the product granules, assessment of the upper limit of the "dichloride" phase is difficult, although an estimated limit of $ZrCl_{1.75(5)}$ is reasonable in light of available data.

Transport and properties of pure $ZrCl_{1.7}$

This phase was finally obtained in pure form only by transport in a temperature gradient. Reaction conditions and yields are given in Table 5. Electron microprobe analyses on several ferns and platelets from the 42-day reaction gave Cl/Zr=1.75(5) with no obvious relationship between crystal form and composition. (A pellet of composition $ZrCl_{1.46}$ was used as the reference standard.)

One of the apparently more important factors controlling both yield and product morphology is the temperature at the hot end, where $ZrCl_4(g)$ is apparently reduced to $ZrCl_3(g)$ and/or $ZrCl_2(g)$ by the $ZrCl/ZrCl_{1.6}$ solid phase mixture. Average autogenous $ZrCl_4(g)$ pressures are estimated to vary from 1 atm for a hot-end temperature of 700° to greater than 20 atm at 850°. Interestingly, no transport occurs (even in a 900°/600° gradient) from a ZrCl/Zr mixture ($P_{900°}$=1 atm of $ZrCl_4$).

The transport rate has been observed to vary from 1-15 mg per week and seems to be greatest for a hot-end temperature of 750°. In all cases reaction tubes were inclined 10-30° from the horizontal to encourage convection in the gas phase. Deposition zones never exceeded 5 cm ($\Delta t < 50°$) implying a rather limited activity range for $ZrCl_4(g)$ and possibly also a fairly small homogeneity range for the depositing phase.

As indicated in Table 5, the platelet form seems to dominate for

Table 5. Some attempts to transport the $ZrCl_{1.7}$ phase

Starting Material (Cl/Zr)	Temperature Gradient	Reaction Time, P[a] (days,atm)	Tube Length (cm)	Product Zone (cm from hot end)	Product Yield (mg)	Crystal Morphology[b]
1.16	700°/550°	7, <1	28	27-28	1	p
1.5	700°/600°	7, 1	28	26-28	1	p
1.35	750°/600°	35, 5	28	10-15	40	f,p,g
1.35	750°/600°	16, ?	20	14-17	10	f,p
1.6	750°/650°	42, ?	18	16-18	100	f,p
1.3	780°/650°	7, ?	20	17-20	5	f,p
1.4	800°/625°	6, 10	27	10-14	5	f,p
1.4	850°/700°	5, >20	26	10-15	5	p

[a]Calculated from the mass of recovered $ZrCl_4$(s) and the "average" temperature.

[b]Abbreviations: p=platelet, f=fern, g=gem-like; listed in decreasing order of abundance.

products transported from $700^{\circ} \geq t(\text{hot-end}) \geq 800^{\circ}$, while under intermediate conditions a fern-like growth pattern is more common. For reactions with hot-end temperatures around 700°, very small (< 0.5 mm diameter) platelets deposit at the cold end but in less than 1 mg yields. However, in the 850° reaction, much larger (some 1-2 mm in diameter) paper-thin hexagonal platelets grow on or near the solid at the hot end. In fact some of these crystals are so thin that they transmit red light under the microscope; grinding this phase leaves a pink tinge on the mortar.

For intermediate conditions, there is frequently a steady morphological change across the deposition zone with very thin platelets near the hot end fading into platelets with fern-like patterns, then into ferns which thicken until branches have a triangular cross section. Similar spire-like growth has also been observed from the sides of thick triangular platelets.

Oscillation photographs of spires and ferns have shown them to be polycrystalline, whereas the thin parallepiped platelets (with 60° and 120° interedge angles) are single with a spindle axis repeat of 3.38 Å. However, zero and first level photographs show very bad streaking parallel to the translation axis. The implication of two-dimensional disorder parallel to the platelet face is further supported by banding between certain pairs of reflections in powder patterns of microcrystalline products.

An excellent quality powder pattern (Appendix Table A-4) of this phase at its lower limit ($ZrCl_{1.6}$) has been obtained from the jet-black macrocrystalline platelet product of a 35-day biphasic equilibration of

microcrystalline $ZrCl_3$ with excess $ZrCl_{1.2}$ at 600°. The development of macrocrystalline platelets by reduction of microcrystalline $ZrCl_3$ hints at a growth mechanism which may involve recrystallization from the gas phase.

Indexing this $ZrCl_{1.6}$ powder pattern on a hexagonal cell with $\underline{a}$=3.3830(2) and $\underline{c}$=19.390(1) was accomplished by using preliminary data from oscillation and Weissenberg photographs of transported $ZrCl_{1.7}$ platelets. Although the structure of this phase is unknown, the unit cell dimensions are quite reasonable for a 3-slab MX_2 structure possibly similar to 3s-$Nb_{1+x}S_2$ ($0.12 < x < 0.25$) which is trigonal (space group R3m) with $\underline{a}$=3.33 Å and $\underline{c}$=17.9 Å (57). The only three observed reflections (100, 008, and 109) which break the rhombohedral extinction conditions in the powder pattern of $ZrCl_{1.6}$ (Appendix Table A-4) are absent in transported $ZrCl_{1.7}$ products.

If interlayer coordination about Zr is assumed to be trigonal antiprismatic, as is the case for all binary zirconium halides of known structure, then the only 3-slab sequences possible are abc bca cab and abc acb cab. The fact that no powder pattern simple enough to represent a 1s-MX_2 structure (abc abc ...) has ever been observed indicates preference for trigonal prismatic coordination about halogen. Hence, of the two proposed sequences, the first seems most feasible for the postulated $Zr_{1+x}Cl_2$($0.15 < x < 0.25$) structure.

The Monohalides

The preparation and structure of ZrBr

The existence of the hitherto unreported zirconium monobromide was easily confirmed by heating $ZrBr_4$ with a large excess of Zr foil at 800° for a few days. Analysis of the black platelet phase scraped from the foil gave a Br/Zr ratio of 1.02±0.02. Because of the similar physical properties and some resemblance of the ZrBr Guinier pattern to that of ZrCl, an attempt was made to index a Guinier pattern of ZrBr so prepared. The 001 and 110 reflections were easily assigned and preliminary hexagonal lattice parameters determined. However, the calculated powder pattern of ZrBr based on ZrCl positional parameters gave generally poor agreement with the observed pattern.

A consideration of polytypism in a variety of layered MX_2 compounds led to solution of this problem. A trial structure was developed for the alternate (A-C-B) slab stacking sequence by using identical fractional coordinates for halogen but with $z' = 1/3 - z$ for Zr. A comparison of calculated and observed powder patterns for both ZrCl and ZrBr in each of the two possible 3-slab sequences (Table 6) leads to the obvious conclusion that ZrBr does have the alternate stacking and that ZrCl and ZrBr are isotypic but not isostructural.

The structures of ZrCl and ZrBr are similar in their trigonal antiprismatic interlayer coordination about zirconium but opposite in coordination about halogen. This is easily seen in a side-by-side comparison of the layer sequences for these isotypic compounds:

Table 6. Comparison of I_{obs} with I_{calc} for A-B-C and A-C-B ZrX[a]

I_{calc} A-B-C	I_{obs}[b] ZrCl	I_{calc} A-C-B	h k l	I_{calc} A-B-C	I_{obs}[c] ZrBr	I_{calc} A-C-B
12	20	0	1 0 1	0	15	9
1	0	51	1 0 2	1	17	21
100	100	3	1 0 4	100	9	2
8	10	100	1 0 5	0	100	100
11	10	48	1 0 7	5	19	29
50	30	0	1 0 8	47	0	2
5	10	31	1 0 10	11	30	34
8	5	7	1 0 11	7	3	6
4	0	2	1 0 13	0	3	6
5	0	6	1 0 14	9	0	0
9	5	6	1 0 16	6	5	3
4	0	12	1 0 17	0	8	12
4	5	4	1 0 19	6	0	0
5	10	1	1 0 20	2	1	1
3	0	7	1 0 22	5	4	8
2	5	0	2 0 1	0	0	1
0	0	8	2 0 2	0	11	3
17	30	1	2 0 4	18	0	0
2	5	19	2 0 5	0	38	19
3	5	11	2 0 7	1	11	7
13	20	0	2 0 8	12	0	0
2	5	10	2 0 10	3	13	11
3	5	3	2 0 11	2	1	2
2	0	1	2 0 13	0	0	3
2	5	3	2 0 14	5	0	0
7	10	4	2 0 16	4	1	2
	*		2 0 17	0	2	9
3	5	0	2 1 1	0	1	2
0	0	11	2 1 2	0	5	4
24	40	1	2 1 4	23	0	0
3	5	27	2 1 5	0	29	26
	*		2 1 7	2	6	10
	*		2 1 8	20	0	1

[a]Hexagonal fractional coordinates for the A-B-C structure calculations were obtained from the literature (11) and those for the A-C-B structure were derived as described in the text. The hhl reflections have been omitted here because of their total insensitivity to stacking sequence.

[b]Intensities estimated visually. For I_{obs} = *, $\theta > 45^{o}$.

[c]Integrated intensities from a microdensitometer film scan.

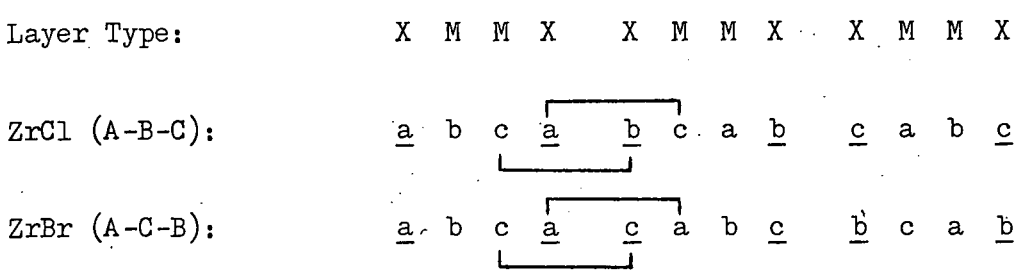

The fact that a recent single crystal study in this laboratory has shown ScCl (58) to be isostructural with ZrBr raised suspicion about the structure type of HfCl. Izmailovich, Troyanov, and Tsirel'nikov (59) recently reported an indexed powder pattern for HfCl along with hexagonal lattice parameters of $\underline{a}$=3.377(2) Å and $\underline{c}$=26.65(2) Å and space group $R\bar{3}m$ from which they inferred isostructuralism with ZrCl. Apparently the possibility of polytypism was not recognized; reflection intensities, although reported to be in good agreement with those of Struss and Corbett (22), were ignored in discussion of the structure. A comparison of powder diffraction intensities from the literature with calculated patterns for both polytypes of HfCl leads to the inescapable conclusion that this compound also adopts the ZrBr (A-C-B) structure. Interestingly, monochlorides of Gd and Tb have recently been shown by single crystal studies to adopt the ZrCl (A-B-C) structure (60).

The non-existence of ZrI

Attempts to prepare ZrI at temperatures up to 900° by providing a large excess of Zr foil or turnings gave $ZrI_{1.8}$ as the most reduced product.

Attempted intercalation of ZrX

The physical properties of ZrCl and ZrBr are reasonable manifestations of their crystal structures. For instance, their graphitic character is clearly related to the weak interslab (van der Waals X-X) interactions and suggests the possibility of intercalation with Lewis acids or bases.

Consideration of a short review of intercalation complexes of Lewis bases and layered sulfides (61) led to selection of ammonia, pyridine, and hydrazine as prime candidates for preliminary work. Heating ZrCl in a sealed Pyrex ampoule with pyridine (distilled from Molecular Sieve) for seven weeks at its boiling point of 115° failed to produce either the physical swelling or detectable lattice parameter changes associated with intercalative processes. A similar treatment of ZrBr for 6.5 weeks also gave negative results as did contact of ZrBr with $NH_3(l)$ for eight days at 25° (P~10 atm) in a thick-wall Pyrex ampoule. Room temperature equilibration of ZrBr with hydrazine for four days in a stoppered vial produced no evidence of intercalation, nor did equilibration with liquid triphenylphosphine at 300° for ten days in a sealed tube.

Attempts to intercalate Na or K into ZrCl at 25° using dry ethylenediamine as a solvent resulted in complete dissolution of the metal after a few hours followed by a bronze coloration of a small portion of the ZrCl not covered by solvent. This bronze material may well be identical to the bronze ZrClH phase recently prepared in this laboratory by reacting ZrCl (even at 25°) with $H_2(g)$ (62).

Intercalation of Lewis acids was also tried. ZrCl was heated at 120°

for 21 weeks in an evacuated, sealed tube with a $Al_2Cl_6(g)$ pressure of a few mm generated by excess $AlCl_3(s)$. X-ray powder data gave no evidence for any kind of reaction. Stirring ZrCl at 25° with a solution of I_2 in CCl_4 again gives negative results, although at 40° an amorphous red-brown product (believed to be ZrI_4) coats the ZrCl after a few hours.

Electrical conductivity

Another physical property of ZrCl and ZrBr which deserves mention is electrical conductivity. Troyanov (48) using presumably single crystals of ZrCl (average size 4x4x0.1 mm), obtained by unspecified methods resistivities of roughly 10^3 ohm·cm perpendicular to the platelets and 10^{-2} ohm·cm parallel to them. Although the values he gives are of questionable precision, the indicated electrical anisotropy is entirely consistent with the structural observation by Adolphson (10) that the metal bilayers in ZrCl parallel the platelet faces.

Further evidence for the high electrical conductivity of both ZrCl and ZrBr has been obtained in this work by two-probe measurements on 1-1.5 g pellets of these phases compressed at 7 Mg/cm^2 to 97% of the theoretical densities. Resistances measured between pellet faces with a VTVM were found to be less than 0.1 ohm for both ZrCl and ZrBr.

X-ray photoelectron spectra of ZrX

X-ray photoelectron spectra of the valence region of these compounds give further evidence for extended delocalization of electrons. The results presented in Figures 2 (ZrCl) and 3 (ZrBr) show a well-developed metallic d band which extends to the Fermi level for both compounds. Data

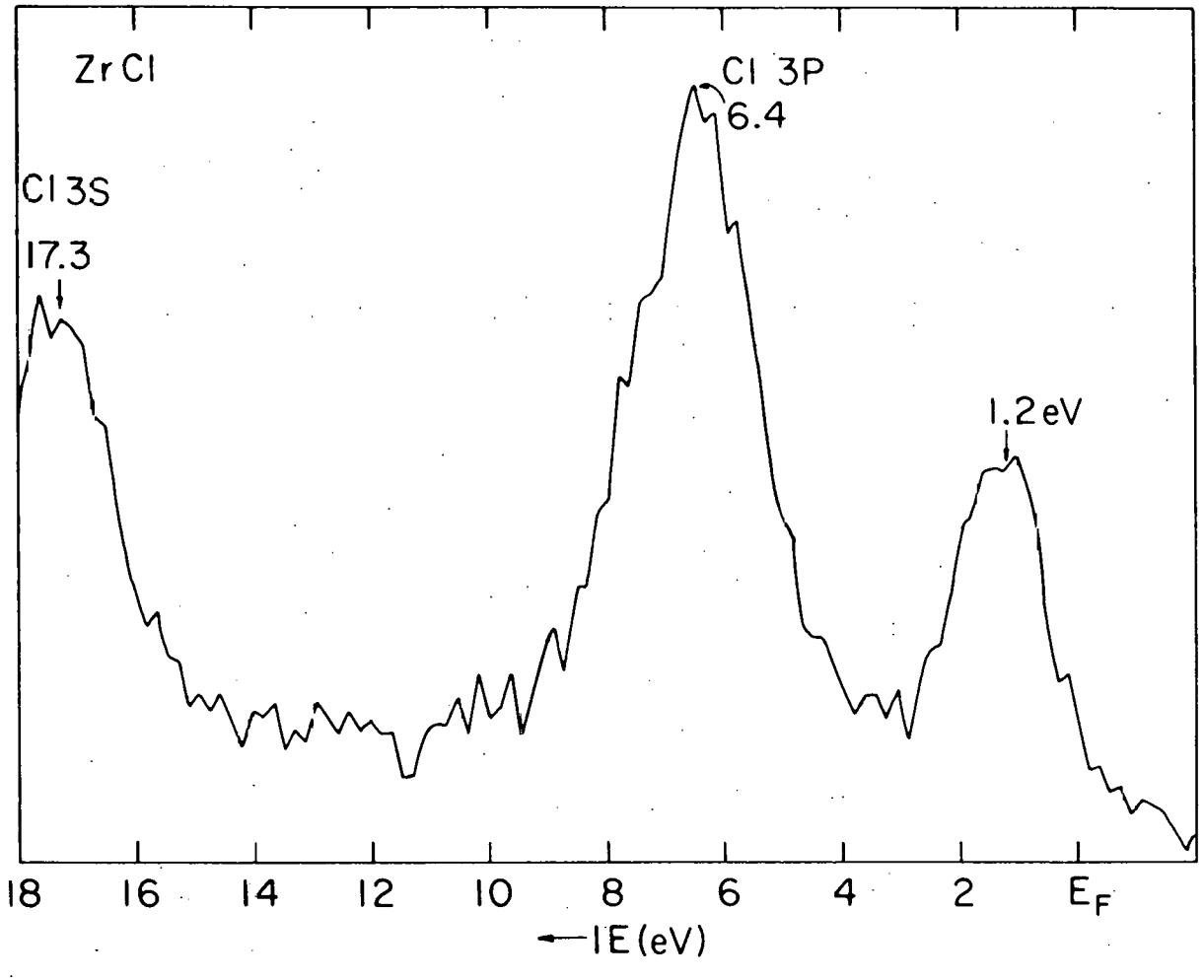

Figure 2. Valence region X-ray photoelectron spectrum of ZrCl

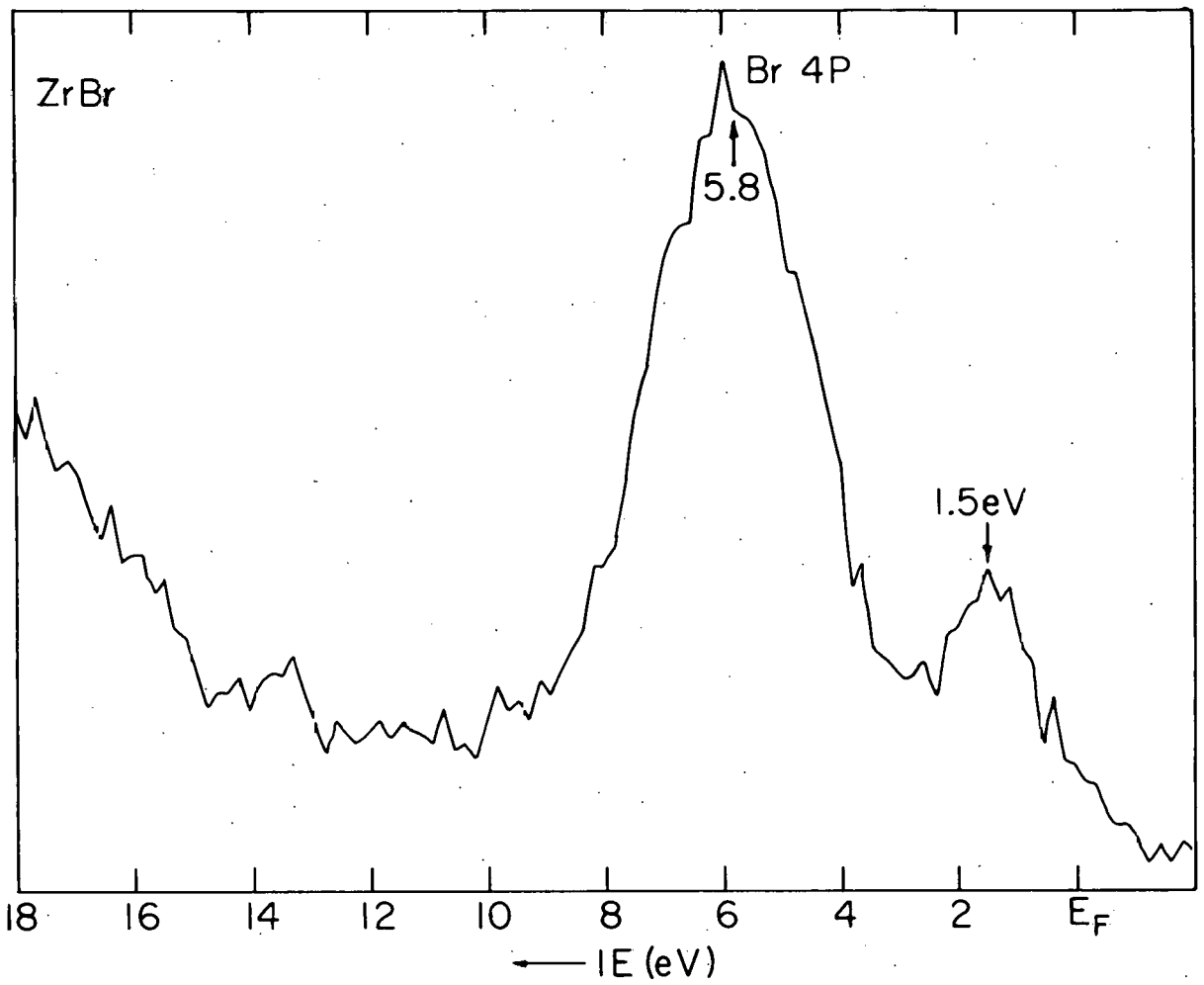

Figure 3. Valence region X-ray photoelectron spectrum of ZrBr

for the valence region are listed together with selected core energies in Table 7.

Both valence and core energies for Zr are slightly (0.3eV) higher in ZrBr than in ZrCl. This is opposite the trend predicted from electronegativity arguments alone, and may reflect the difference in interlayer coordination about halogen. Perhaps the Zr atoms in ZrBr can electrostatically "see" the halogen atoms in the nonadjacent but equivalently positioned second-nearest layer better than in ZrCl where the coordination about halogen is trigonal antiprismatic. It may in fact be this stronger interaction of Zr with second-layer halogen which makes ZrBr structurally less susceptible to grinding damage than is ZrCl (judged from line broadening in Guinier films). Perhaps the increased intralayer X-X distance (3.50 Å in ZrBr compared with 3.42 Å in ZrCl) gives the Zr atoms a larger "window" in ZrBr. In light of the "advantages" of the A-C-B structure, it is indeed puzzling that ZrCl adopts the A-B-C sequence in the first place.

As expected, the Zr valence and core energies in ZrCl are intermediate to those in α-Zr metal and $ZrCl_4$. In the metal, each Zr is surrounded by six intralayer atoms at 3.23 Å (the hexagonal a parameter) and trigonal prismatically by three at 3.18 Å in two neighboring layers. The intralayer M-M distance in ZrCl is considerably greater (3.42 Å) than in the metal while the interlayer M-M separation is smaller (3.09 Å) and indicative of strong metal-metal bonding.

Interestingly, the Cl 2p peaks for ZrCl are significantly sharper than for $ZrCl_4$ while the Zr 3d peaks have a similar width for both compounds. This effect is easily understood from the fact that in $ZrCl_4$ there are

Table 7. X-ray photoelectron peaks (eV) for some zirconium halides

	Zr	ZrBr	ZrCl	$ZrCl_4$[a]
Zr 4d	-	1.5	1.2	(5.0)
Br 4p	-	5.8	-	-
Cl 3p	-	-	6.4	(5.0)
O 2p	-	-	-	-
Cl $3s_{1/2}$	-	-	17.3	15.7
Zr $3d_{5/2}$	177.6[b]	179.6	179.3	182.8[c]
Zr $3d_{3/2}$	180.0	182.0	181.8	185.2
Br $3p_{3/2}$	-	182.6	-	-
Br $3p_{1/2}$	-	189.9	-	-
Cl $2p_{3/2}$	-	-	199.6	198.5
Cl $2p_{1/2}$	-	-	201.2	200.1

[a]Energies for this insulating phase have been corrected for charging effects relative to a few monolayers of a Au standard vaporized onto the sample surface.

[b]Given as 178.5eV in reference 63 relative to a hydrocarbon C1s standard.

[c]This band occurs at 182.6eV in ZrO_2 standardized against the C1s line (285.0eV) of surface deposited hydrocarbons (63).

three unique Zr-Cl distances (2.307 Å, 2.498 Å, and 2.655 Å) and eight different Cl-Cl distances (ranging from 3.30 Å to 3.81 Å) while the chemical environment for all Zr atoms is identical (64). In ZrCl, however, there is only one unique atom of each kind, hence sharp peaks for both Cl 2p and Zr 3d.

Thermal stability of ZrX and reactions with glass

Uchimura and Funaki (39) have shown that up to 900° $ZrCl_4(g)$ is the only detectable $ZrCl_n(g)$ species in the Zr-Cl system. Unfortunately, measurements on the ZrCl/Zr equilibrium were done between 750° and 900° on samples which were directly in contact with glass and the results may therefore be somewhat in error. However, $ZrCl_4(g)$ pressures calculated from their data are within 30% of those determined here by a restricted volume decomposition of ZrCl in Ta at 975° (P_{obs}=2.9 atm, P_{calc}=2.8 atm) and at 1050° (P_{obs}=10.4 atm, P_{calc}=7.2 atm).

ZrCl remains a solid phase even at 1050°. If heated to 1100° (P=15-20 atm) there is still no evidence of melting. In an attempt to contain the > 50 atm pressures expected at 1200°, a sealed 0.4 mm o.d. Ta tube containing ZrCl was placed inside a 6 mm o.d. capped tube along with sufficient ZrCl to produce an intertube pressure of 15 atm of $ZrCl_4(g)$ when completely disproportionated. Even with these precautions, the inner tube ruptured, resulting in the complete disproportionation of its contents. Hence it is only possible to conclude that ZrCl melts at greater than 1100°.

If either ZrCl or ZrBr is heated in a fused silica ampoule at 800-

850° for a few days, the ZrX turns from a blue-black to a bronze color with a considerable broadening of the powder pattern and a general line shift to lower angles. Furthermore, the glass becomes badly etched in areas where it directly contacts the ZrX phase. If however, the sample is first placed in an open Ta boat and heated under the same conditions the powder pattern remains virtually unchanged and the glass unetched.

If ZrX is heated with 0.33 mole fraction ZrO_2 (a net Zr 2+ oxidation state) at 850° for 8 days, fairly sharp powder patterns of $ZrX_{1-x}O_x$ are obtained (mixed with unconsumed ZrO_2) which are qualitatively identical to those obtained by heating ZrX in fused silica. From measurements on the shifted 110 and 001 lines the ZrCl lattice appears to have expanded by approximately 2% in a and 1% in c, whereas for ZrBr the lattice expansions were 1.76% and 1.45%, respectively. The powder pattern of $ZrX_{1-x}O_x$ is of considerable better quality for X=Br than for X=Cl and shows a direct correspondence (in number and intensity) with lines in the ZrBr powder pattern. Precise lattice constants (Appendix Table A-7) of a=3.5646(2) and c=28.479(5) were determined from 22 reflections for $ZrBr_{1-x}O_x$. From a qualitative comparison of ZrO_2 line intensities in powder patterns of the mixture before and after reaction, x is probably less than 0.1. In light of the fact that O^{2-} is usually considered to be smaller than Cl^-, the expansion of both lattice parameters of $ZrX_{1-x}O_x$ relative to those of ZrX is probably the result of extraction of electron density from the Zr-Zr bilayer. X-ray photoelectron spectra of these materials would be very helpful in testing this hypothesis.

THE CRYSTAL STRUCTURE OF $Zr_6Cl_{12}Cl_{6/2}$

Structure Determination

Initial positions for one general (96-fold) Zr and two general Cl sets, Cl(I) and Cl(II), were obtained from the electron density map output by MULTAN (65) for input to ORFLS (66). Five cycles of least-squares refinement produced a conventional residual of 0.21.

Although a preliminary electron microprobe analysis[1] had suggested the composition $ZrCl_{2.2}$, examination of the electron density map generated by the program ALFF (67) revealed a new 48-fold set of Cl-size peaks belonging to special set g in the selected space group. Subsequent electron microprobe analyses on two very small (0.01-0.02 mm) gem crystals gave Cl/Zr=2.5(2).

Inclusion of this Cl(III) set among the atoms input to ORFLS yielded a residual of 0.137 after three cycles. Anisotropic refinement (with appropriate restrictions on the special set) resulted in R=0.113 and R_w=0.125. The program Omega (67) written locally by C. R. Hubbard was then used to reweight the dataset. The final refinement converged after

---

[1]Only two of the 15-20 crystals of this transported phase were considered large enough (diameter > 0.03 mm) for single crystal work; both were mounted successfully. The crystal on which X-ray diffraction data had not been collected was demounted, washed with trichloroethylene to remove the silicone grease, and used for a preliminary electron microprobe analysis.

three cycles at R=0.111 and R_w=0.096 with no shift/error greater than 0.01. Final atomic parameters are given in Table 8 while a listing of observed and calculated structure factors appears in Table 9.

The final difference map was flat to ±1 electron/A^3 except for a peak of maximum height seven electrons/A^3 at the cluster center (16-fold special position a). The size and shape of this peak represents roughly 3-5 electrons per cluster and may simply be the result of program termination errors. It is interesting that small residual peaks are frequently observed at the center of phenyl rings in structure solutions of organic and organometallic compounds (68) as well as in metal cluster compounds (69). Although the final agreement factor can be improved by putting a carbon atom at the cluster center (refined B=2.2 A^2), there is no clear justification for doing so in this case. However, this possibility cannot be disproved from available data either since the electron microprobe analyses would not have detected elements lighter than sodium. Furthermore, the observation of this phase in only one of eight transport attempts (Table 5), and then in extremely small yields, does leave some suspicion that this compound could be an impurity stabilized phase.

Interatomic distances and angles

Pertinent interatomic distances and angles with associated standard deviations were calculated by the program ORFFE (70) using as input the variance-covariance matrix from the final refinement cycle of ORFLS (66). These results are presented in Table 10 along with corresponding values for $TaCl_{2.5}$. It is unfortunate that the isostructuralism of these two

Table 8. Final atomic parameters for Zr_6Cl_{15}

A. Fractional coordinates for the independent atoms

Atom	Ia3d Set	x	y	z
Zr	96(h)	0.06137(10)	0.96548(11)	0.08092(12)
Cl(I)	96(h)	0.15685(29)	0.02965(31)	0.05084(32)
Cl(II)	96(h)	0.10939(32)	0.87617(30)	0.01907(28)
Cl(III)	48(g)	0.57115(63)	0.25-x	0.12500

B. Anisotropic temperature factors ($Å^2$)

Atom	$10^5\beta_{11}$	$10^5\beta_{22}$	$10^5\beta_{33}$	$10^5\beta_{12}$	$10^5\beta_{13}$	$10^5\beta_{23}$
Zr	149(7)	145(7)	136(6)	6.5(4.6)	5.6(4.5)	16(4)
Cl(I)	133(17)	228(18)	225(19)	-20(12)	-35(12)	66(14)
Cl(II)	200(17)	176(15)	176(17)	43(13)	-23(12)	12(13)
Cl(III)	182(15)	182(15)	209(25)	-78(18)	-35(12)	-35(12)

Table 9. Observed and calculated structure factors for Zr_6Cl_{15}

H = 2		
K	L	FO	FC
1	1	88	92
2	0	1730	1720

H = 3		
K	L	FO	FC
2	1	282	287
3	2	274	282

H = 4		
K	L	FO	FC
0	0	327	454
2	2	326	434
3	1	86	92
4	0	618	724
4	4	811	736

H = 5		
K	L	FC	FC
3	2	372	391
4	1	532	560
5	2	962	1048

H = 6		
K	L	FO	FC
1	1	124	156
2	0	560	699
3	1	323	334
3	3	760	815
4	0	189	209
5	3	804	863
5	5	630	673
6	4	705	668

H = 7		
K	L	FO	FC
2	1	102	146
3	2	132	161
4	1	270	292
4	3	1145	1198
5	2	453	472
5	4	810	835
6	1	581	621
6	5	319	325
7	2	1013	1044
7	6	240	240

H = 8		
K	L	FC	FC
0	0	983	1112
2	0	336	355
2	2	556	693
3	1	112	154
4	0	203	267
5	1	256	269
5	3	588	590
6	0	510	509
6	2	429	381
6	6	84	127
7	1	347	356
7	3	77	70
7	5	222	216
8	0	952	922
8	4	79	67
8	6	412	391

H = 9		
K	L	FO	FC
2	1	419	458
3	2	423	443
4	1	468	483
4	3	396	405
5	2	114	155
5	4	421	416
6	1	274	269
6	5	110	135
7	2	76	88
7	4	463	432
8	1	619	612
8	3	127	163
8	7	617	539
9	2	767	736
9	6	308	304

H = 10		
K	L	FO	FC
1	1	245	240
2	0	544	615
3	1	302	320
3	3	648	640
4	0	395	416
5	1	140	167
5	3	89	113
5	5	142	170
6	0	314	290
6	2	501	489
7	1	674	666
7	3	266	281
7	5	194	201
7	7	284	280
8	0	223	230
8	2	469	468
8	4	77	96
8	6	98	158
9	1	250	239
9	3	439	417
9	7	83	111
9	9	755	661
10	0	381	393
10	4	83	134

H = 11		
K	L	FO	FC
3	2	812	825
4	1	551	561
4	3	118	139
5	2	228	225
5	4	238	246
6	1	325	313
6	3	434	400
7	2	244	260
7	6	91	99
8	3	299	280
8	5	366	342
8	7	79	51
9	2	85	125
9	4	432	410
9	6	128	159
9	8	211	212
10	1	331	316
10	3	90	119
10	7	617	531
10	9	68	62
11	2	265	243
11	6	706	650

H = 12		
K	L	FC	FC
0	0	355	376
2	0	107	141
2	2	475	425
3	1	616	629
4	0	394	347
4	4	532	502
5	1	452	428
6	2	75	57
6	4	167	197
6	6	455	473
7	1	67	131
7	3	73	97
8	4	323	343
8	6	166	177
8	8	430	421
9	1	461	435
9	3	152	212
9	5	143	170
10	0	75	89
10	2	336	338
10	8	106	131
10	10	175	163
11	1	217	246
11	7	84	100
11	9	149	198
12	0	544	521
12	8	539	442
12	12	127	120

H = 13		
K	L	FO	FC
3	2	82	123
4	1	577	555
4	3	437	402
5	2	612	560
5	4	272	264
6	1	177	191
6	3	346	340
6	5	192	208
7	2	75	75
7	6	102	127
8	1	319	309
8	3	116	174
8	5	94	85
8	7	409	360
9	2	94	123
9	4	390	361
9	6	303	282
9	8	332	308
10	1	302	293
10	5	428	382
10	7	127	145
11	2	95	92
11	4	479	430
11	6	316	295
11	8	586	513
12	3	84	105
12	5	185	218
12	7	250	247
12	9	375	316
13	6	253	221
13	10	292	254

H = 14		
K	L	FO	FC
1	1	256	247
3	1	287	297
4	0	431	419
4	2	470	419
5	1	84	84
5	3	207	224
6	0	165	177
6	4	315	329
7	1	166	209
7	3	91	131
7	7	202	223
8	2	166	218
8	6	260	271
9	5	493	428
9	7	120	134
10	2	329	301
10	6	284	265
10	8	76	71
11	3	292	261
11	9	135	153
11	11	99	104
12	0	78	113
12	2	89	133
12	6	401	326
12	8	112	147
12	10	130	147
13	1	88	98
13	3	88	98
13	5	82	88
13	7	271	263
13	11	99	107
14	0	392	368
14	4	181	207
14	8	371	284
14	12	106	175

H = 15		
K	L	FO	FC
2	1	404	401
3	2	317	302
4	1	439	433
4	3	539	501
5	2	465	434
5	4	301	295
6	1	496	466
6	3	102	89
7	2	103	104
7	6	278	286
8	5	206	198
8	7	130	167
9	4	105	64
9	6	392	354
10	3	202	209
10	5	351	331
10	7	121	139
10	9	75	112
11	4	104	151
11	10	97	108
12	1	100	130
12	3	389	372
12	9	94	59
13	2	87	137
13	4	379	320
13	6	94	98
13	8	121	143
14	1	112	170
14	5	106	120
14	7	318	276
14	9	123	142
15	6	208	214
15	10	98	89

H = 16		
K	L	FO	FC
3	1	77	114
4	2	248	250
4	4	336	330
5	1	145	188
6	0	600	530
6	4	102	133
6	6	396	385
7	1	123	181
8	0	354	319
8	8	95	154
9	1	309	301
9	3	187	193
9	7	255	236
10	0	512	445
10	2	241	247
10	6	83	80
10	8	246	237
11	1	289	279
11	5	372	315
11	9	101	133
12	2	459	393
12	6	372	314
12	8	190	180
12	12	165	217
13	1	106	144
13	5	91	74
14	0	131	176
14	2	100	139
14	6	306	262
14	10	94	96
16	0	121	159

H = 17		
K	L	FC	FC
2	1	89	90
3	2	351	357
4	1	278	284
5	2	193	203
5	4	107	149
6	1	122	156
6	3	117	164
6	5	103	115
7	6	88	92
8	1	382	339
8	7	253	234
9	2	85	102
10	3	546	488
10	5	426	375
11	4	415	357
11	6	94	134
11	10	81	98
12	1	292	285
12	3	86	114
12	5	130	182
12	7	159	166
12	9	89	90
13	6	179	206
13	8	89	82
13	12	90	70
14	1	123	185
14	5	89	79
14	9	176	196
14	11	184	190
16	5	90	83
16	7	130	151
17	6	133	145

H = 18		
K	L	FO	FC
2	0	92	138
3	3	94	120
4	0	103	121
5	5	96	141
6	0	367	292
6	2	511	449
6	4	99	140
7	1	90	104
7	3	120	181
8	0	282	270
8	2	240	235
8	4	261	257
9	1	301	296
9	9	203	202
10	0	204	222
10	2	175	192
10	6	380	337
11	1	173	208
11	7	184	183
11	11	125	129
12	0	417	390
12	8	212	203
14	0	86	120
14	2	278	282
14	6	107	151
14	8	93	52
14	10	146	151
15	5	108	144
16	0	143	168
16	2	85	67
16	4	113	126
17	3	270	262

H = 19		
K	L	FO	FC
5	4	75	42
6	1	308	271
6	3	107	167
7	2	130	172
7	4	86	107
7	6	428	352
8	1	142	194
8	3	125	165
8	5	449	385
9	2	88	63
9	6	79	100
10	1	269	250
10	3	112	116
10	7	339	301
10	9	108	103
11	2	115	136
11	6	160	168
11	10	129	152
12	3	101	125
12	5	213	223
12	7	84	69
12	9	114	147
12	11	109	134
13	4	121	160
14	5	96	107
16	3	120	182

H = 20		
K	L	FO	FC
0	0	642	551
2	0	120	142
2	2	85	130
3	1	469	459
5	1	493	441
6	0	155	188
6	2	86	86
6	4	166	187
6	6	103	81
7	1	106	141
7	5	308	292
8	0	109	125
8	2	86	107
9	3	169	199
12	6	89	105
13	7	123	124
14	0	91	125
14	4	119	154

H = 21		
K	L	FO	FC
3	2	85	117
8	1	170	180
8	5	117	147
8	7	124	130
9	4	103	98
9	8	93	107
10	7	256	239
11	8	106	125
12	1	89	39
12	3	90	119

H = 22		
K	L	FC	FC
2	0	96	178
4	0	131	184
5	1	420	388
5	5	298	302
6	2	99	91
6	4	83	91
7	3	177	173
7	7	165	240
8	4	134	172
9	5	149	204
11	5	95	104
12	0	97	134

H = 23		
K	L	FC	FC
6	1	122	155
6	3	117	159
8	1	111	152
8	5	113	152

H = 24		
K	L	FC	FC
4	0	105	121
4	2	86	78
6	0	140	193
6	4	102	127

H = 25		
K	L	FO	FC
2	1	126	186

Table 10. Interatomic distances (Å) and angles for M_6Cl_{15} (M=Zr,Ta)[a]

Intracluster interatomic distances

Type	Zr_6Cl_{15}	Ta_6Cl_{15}	Type	Zr_6Cl_{15}	Ta_6Cl_{15}
M - M	3.199(4)	2.921(4)[b]	I - I	3.529(12)[b]	3.495(17)
	3.215(4)	2.928(4)[b]	II - II	3.518(6)[b]	3.408(17)
M - I	2.506(6)[b]	2.427(12)[b]	I - II	3.462(9)	3.275(17)
	2.514(7)[b]	2.436(12)[b]		3.609(10)	3.454(17)
M - II	2.494(6)	2.413(12)	I - III	3.306(12)	3.217(28)
	2.511(6)	2.462(12)		3.510(10)	3.353(28)
M - III	2.588(5)	2.564(25)	II - III	3.359(7)	3.163(28)
				3.572(7)	3.393(28)

Intracluster angles[c]		Intercluster M-III-M angle	
Zr-I-Zr	79.2(2)°	M	angle
Zr-II-Zr	79.9(2)°	Zr	138.5(4)°
Zr-Zr(trans)-III	175.8(2)°	Ta	142.0°
I-Zr-II	169.1(2)°		

[a]Results for Ta_6Cl_{15} are from reference 14. Abbreviations: I=Cl(I); II=Cl(II); III=Cl(III).

[b]These pairs of distances are equal within given standard deviations.

[c]These angles are not available for Ta_6Cl_{15}.

compounds was not discovered until final stages of the Zr_6Cl_{15} refinement.

Discussion

Zr_6Cl_{15} is the first M_6 cluster compound reported for the Group IVB transition metals. Unlike the isostructural Ta_6Cl_{15} (14) which has been shown by Kuhn and McCarley (71) and recently confirmed by Schäfer and Giegling (72) to be the most reduced compound in the Ta-Cl system, Zr_6Cl_{15} is the middle of five compounds in the Zr-Cl system. Perhaps a very narrow stability range and/or extreme kinetic problems in forming this line compound contribute to its rare appearance. Even attempts to prepare this elusive phase stoichiometrically from ZrCl and $ZrCl_4$ or by a restricted volume decomposition of $ZrCl_3$ have not produced Zr_6Cl_{15} observable in powder patterns.

Essentially the M_6Cl_{15} (M=Zr,Ta) structure consists of an infinite 3-dimensional linkage of $M_6Cl_{12}^{3+}$ groups via intercluster bridging chlorides--in conventional symbolism, $(M_6Cl_{12}^{i})Cl_{6/2}^{a-a}$ (i for German inser and a for auser). In contrast to Nb_6F_{15} (73) and Ta_6I_{15} (74) both of which crystallize in space group Im3m with Z=2 and have six near neighbor clusters, Zr_6Cl_{15} (Z=16) has eight near neighbor clusters but is bridge-bonded to only six of them. The Nb_6F_{15} structure can be thought of as two interpenetrating and parallel cluster networks with all $M\text{-}X^{a-a}\text{-}M$ bond angles precisely 180°, whereas in Ta_6Cl_{15} and Zr_6Cl_{15} these angles are 142.0° and 138.5°, respectively, with all clusters linked into a single infinite network.

While the M_6 groups in Nb_6F_{15} and Ta_6I_{15} form a perfectly regular

octahedron surrounded by a regular cube of X^i atoms and a perfect X^{a-a} octahedron, the precise local 4-fold symmetry is lost in M_6Cl_{15} (M=Zr,Ta) while the 3-fold and lower symmetry is retained. Perhaps the most outstanding feature of the M_6Cl_{15} structure is the presence of four sets of symmetry related but nonintersecting 3-fold axes on which all clusters are centered. Furthermore, near neighbor clusters which have no common bridging chlorine atoms always occur along a common 3-fold axis.

In all of the M_6X_{15} cluster compounds, each X atom bridges two and only two metal atoms--either intracluster (X^i) over an M_6 pseudo-octahedral edge or intercluster (X^{a-a})--while each M is bonded to four other intracluster M-atoms as well as to four X^i and one X^a. All clusters in Zr_6Cl_{15} are structurally identical and positionally interconvertible by symmetry. An ORTEP (75) generated drawing of the cluster centered at (0,0,0) is shown in Figure 4 as viewed down one of the three symmetry-equivalent cell axes. As in Ta_6Cl_{15}, the approximately octahedral Zr_6 group sits inside a distorted cube defined by the twelve Cl^i atoms--one approximately centered on each cube edge--with a Zr atom displaced from the center of each face by approximately 0.24 Å toward the cluster center resulting in a Cl_I-Zr-Cl_{II} angle of 169°. Whereas the M_6 group in Ta_6Cl_{15} is precisely octahedral within the error limits given by Bauer and von Schnering (14), the Zr_6 group in Zr_6Cl_{15} is slightly elongated along a unique three-fold axis. The average Zr-Zr distance of 3.207 Å is considerably longer than the Ta-Ta distance of 2.924 Å, but approximately equal to the average M-M distance of 3.205 Å in α-Zr (6 neighbors at each 3.179 Å and 3.231 Å). It is especially interesting that $ZrCl_3$ has a much

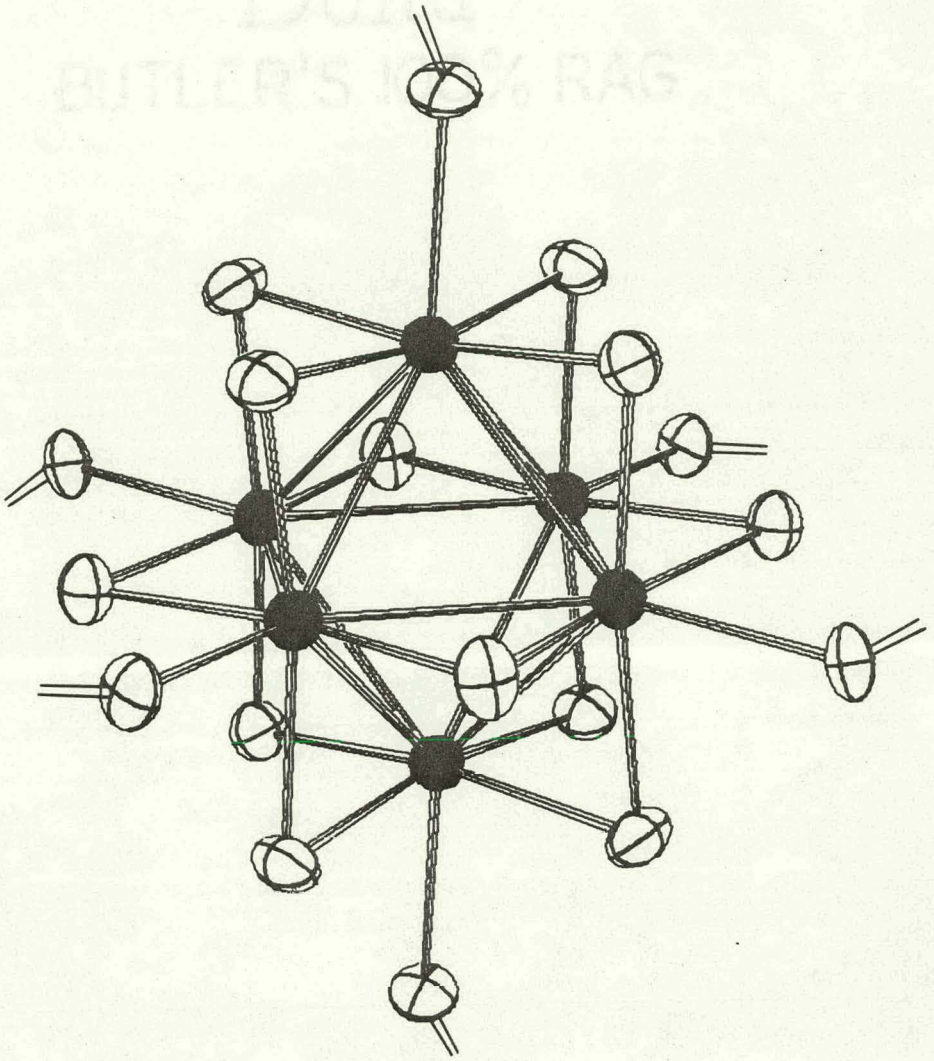

$Zr_6Cl_{12}Cl_{6/2}$

Figure 4. Cluster centered at (0,0,0), viewed down [001]

shorter Zr-Zr separation (3.07 Å) than Zr_6Cl_{15} but an almost identical crystallographic density.

An electron count shows the M_6 group of Zr_6Cl_{15} to have nine bonding electrons as opposed to fifteen for Ta_6Cl_{15}. According to the molecular orbital scheme proposed by Cotton and Haas (76) for the isolated $M_6X_{12}^{n+}$ group, eight of these electrons would go into the A_{1g} and T_{1u} bonding molecular orbitals leaving one unpaired electron in either the A_{2u} or T_{2g} bonding molecular orbital, whichever is of lower energy. Bauer and von Schnering (14) have used magnetic measurements to confirm the presence of one unpaired electron per cluster in the 15-electron Ta_6X_{15} (X=Cl,Br) compounds. Attempts in this laboratory to obtain sufficient quantities of Zr_6Cl_{15} for similar measurements have been unsuccessful. Perhaps with six fewer bonding electrons per cluster than Ta_6Cl_{15}, $ZrCl_{2.5}$ may be stable with respect to disproportionation to $ZrCl_{1.8}$ and $ZrCl_3$ only under extremely limited conditions and may not even exist at temperatures where kinetic hindrance to preparation of this phase is not dominant.

FUTURE WORK

In addition to determination of precise lattice constants for ZrX_3 (X=Cl,Br,I) and confirming the nonstoichiometry of these phases, the present work has resulted in the identification and X-ray characterization of several new, or hitherto poorly characterized zirconium subhalides. While the basic aims of this work have been accomplished, there remain a number of possibilities for future work on the Zr-X systems. Furthermore, some of the results obtained as well as techniques developed in the course of this work suggest possible research on related systems.

First, some long-term (perhaps many months) biphasic equilibrations are needed to determine composition limits for the $ZrBr_{1.8}$ phase and the upper composition limit of both the $ZrCl_{1.7}$ phase and the diiodide. A more precise determination of the triiodide lower limit and a more detailed study of the lattice parameter variation across the composition range of the triiodide are also needed.

Recent studies on the stress corrosion cracking of the nuclear fuel rod material Zircaloy-2 by fission-product iodine and cesium have suggested that chemical reactions can nucleate cracks in smooth specimens (77). Hence attainment of structural and thermodynamic data on the $ZrI_{1.8}$ phase is clearly essential for a better understanding of the nature of this chemical corrosion.

Second, perhaps transporting agents such as those employed by Schäfer (e.g., $AlCl_3$, $GaCl_3$, $FeCl_3$) (78) in growing crystals of various transition

metal subchlorides can be used to improve yields of $ZrCl_{1.7}$ and Zr_6Cl_{15}. Other transition metals (e.g., Re, Nb, etc.) which are known to form gaseous subhalide molecules might also serve to provide more "reducing power" in the deposition zone. In either case, the object is to provide gaseous subhalide species which can either reduce $ZrCl_4(g)$ or aid in disproportionation of $ZrCl_n(g)$ species to $ZrCl_4(g)$ and the depositing solid phase.

In the Zr-Br and Zr-I systems there has been no obvious transport of phases more reduced than the trihalides. However, a few ($\sim$0.05 mm diameter) gem-like crystals have been observed in a Zr-I system reaction when pacification of the metal prevented complete reduction to the diiodide lower limit ($ZrI_{1.8}$). The nearly perfect shape of these multi-faceted crystals implies growth from the gas phase. Although no analytical data are available, these "gems" may represent a cluster compound like Ta_6I_{15} (74), Ta_6I_{14} (71,79), or Nb_6I_{11} (80,81). Since Ta_6Br_{15} has been shown from powder data (14) to be isostructural with Ta_6Cl_{15}, perhaps Zr_6Br_{15} can also be prepared under appropriate conditions.

Third, the inertness of Ta to Zr subhalides at temperatures where reaction with glass is troublesome, suggests that accurate static thermodynamic measurements on the ZrX/"ZrX_2" and Zr/ZrX equilibria can be carried out in glass providing the subhalides and/or metal are contained in Ta or some other suitably inert container. As noted earlier in this work, the powder patterns obtained for ZrX (X=Cl,Br) do not deteriorate when heated to 850° for several days in an open Ta boat sealed in fused silica, nor does the glass become etched. This simple modification of the

apparatus employed by Uchimura and Funaki (39) in their thermodynamic study of the Zr-Cl system would not only increase the reliability of the data, but would also permit longer reaction times in order to obtain more crystalline products for X-ray identification.

Fourth, it may be possible to prepare ternary phases of the type $M_xZr_6X_{18}$ or $M_xZr_6I_{14}$ with isolated $Zr_6X_{18}^{n-}$ (X=Cl,Br) or $Zr_6I_{14}^{n-}$ cluster anions by appropriate choice of counter cation salts. Simon, von Schnering, and Schäfer (82) have reported easy preparation of up to 1 mm diameter gem-like crystals of $K_4Nb_6Cl_{18}$ in 1.5 g yields by reduction of Nb_3Cl_8 with Nb in a KCl/LiCl eutectic melt. They also have employed a stoichiometric solid-solid reaction by heating a pressed pellet of composition $4KCl + Nb_6Cl_{14}$ and have similarly made the isostructural $K_4Nb_6Br_{18}$. In light of the fact that both Cs and I are ^{235}U fission products, the Cs-Zr-I ternary system should perhaps receive special attention.

Fifth, the easy preparation of ZrBr immediately suggests the probable existence of the hitherto unreported HfBr. If this compound can be prepared, it would also be of interest to determine whether it adopts the ZrCl (A-B-C) or the ZrBr (A-C-B) structure. Similar work on the Ti-X and Th-X systems might also prove fruitful.

Sixth, using the technique described in this work ($MX + MX_4$), it may be possible to prepare high purity HfX_3 (X=Cl,Br), a task which Dahl, et al. (15), found "unrewarding" when employing Hf powder. This HfX_3 could in turn be used to explore the intermediate region via biphasic equilibrations with HfX.

Seventh, "dissolution" of oxygen by ZrX (X=Cl,Br) to give $ZrX_{1-x}O_x$ products which evidently retains the ZrX structures, suggests the possible existence of $ZrX_{1-x}S_x$ and other ternary substitution compounds of ZrX, HfX, etc. Further research into the ternary Group IVB-halogen-chalcogen systems might well open some new doors for future work.

APPENDIX

Table A-1. Guinier powder pattern of $ZrI_{1.8}$

d_{obs}	I_{obs}[a]	d_{obs}	I_{obs}	d_{obs}	I_{obs}
7.45	2	2.054	1	1.4272	1
6.45	1	2.044	1	1.4186	1
6.22	1	2.205	1	1.4088	1
3.722	1	1.9428	10*-	1.3769	2
3.631	1	1.9275	3*+	1.3688	1
3.418	1	1.9200	Si	1.3650	1
3.383	1	1.9072	1	1.3577	Si
3.328	4	1.9007	1	1.3438	1
3.243	4	1.8713	10*-	1.3419	1
3.206	2	1.8641	1	1.2824	4*-
3.137	Si	1.8145	1	1.2776	4
3.102	2	1.8095	1	1.2566	1
3.056	6*-	1.7539	1	1.2456	Si
3.004	6*-	1.7232	1	1.2430	2
2.949	5*-	1.6969	1	1.2407	1
2.859	1	1.6903	1	1.2230	1
2.813	2	1.6716	1	1.2142	2
2.796	2	1.6684	1	1.2106	3*+
2.738	3	1.6631	2	1.2071	2
2.677	1	1.6573	1	1.1960	1
2.643	1	1.6372	Si	1.1912	2
2.591	1	1.6305	2	1.1862	1
2.522	1	1.6264	1	1.1773	1
2.514	1	1.6206	2	1.1574	1
2.487	1	1.6021	2	1.1509	1
2.475	2	1.5847	1	1.1415	1
2.438	2	1.5786	1	1.1347	1
2.388	2	1.5575	1	1.1241	1
2.331	1	1.5160	1	1.1088	Si
2.275	1	1.5433	1	1.1032	1
2.248	1	1.5261	1	1.1001	1
2.205	1	1.5012	1	1.0973	1
2.176	1	1.4721	1	1.0942	2
2.159	1	1.4447	2	1.0917	2
2.139	1	1.4383	1		

[a]Indication of pronounced attenuation (*-) or enhancement (*+) of certain reflections by preferred orientation was judged relative to a Guinier pattern of six macroscopic (0.5-1.5 mm diameter) platelets of this phase mounted in the same fashion as a powdered sample, but with special care taken to assure that all platelets were firmly affixed parallel to the tape.

Table A-2. Guinier powder pattern of $ZrBr_x$ mixed with unreacted ZrBr[a]

d	I_{obs}	I_{ZrBr}[b]	d	I_{obs}	I_{ZrBr}	d	I_{obs}	I_{ZrBr}
7.31	8		2.160	4		1.4558	1	
6.81	3		2.096	1		1.4505	1	1
4.976	1		2.061	2	3	1.4374	1	
4.322	4		2.003	1		1.4312	1	
4.010	2		1.9738	1		1.4234	1	
3.924	3		1.9201	Si		1.4185	1	
3.397	4		1.8894	8		1.4060	1	
3.211	3		1.8818	8		1.4017	2	2
3.136	Si		1.7804	4		1.3898	2	
3.095	2		1.7529	6	5	1.3712	2	
3.077	6		1.7222	1		1.3597	Si	
3.021	2	2	1.7111	1		1.3346	2	1
2.970	2	2	1.6408	1		1.3327	4	
2.815	3		1.6371	Si		1.3234	1	
2.714	2		1.6115	1		1.3085	1	
2.670	10	10	1.6068	2		1.2458	Si	
2.589	3		1.6045	1		1.2271	2	
2.566	3		1.5782	1		1.2237	2	
2.483	3		1.5677	1		1.2208	3	
2.459	1		1.5560	1		1.1939	5	
2.427	1		1.5452	1		1.1903	5	
2.422	1	2	1.5372	5		1.1240	2	3
2.331	3		1.5280	1		1.1087	Si	
2.286	1		1.5087	1		1.0923	2	
2.278	2		1.4875	2		1.0880	2	
2.275	2		1.4805	2		1.0865	1	
2.263	1		1.4652	2	4			

[a] Net composition: $ZrBr_{1.32}$; $1.4 < x < 1.6$ (estimated).

[b] Intensities for lines of pure ZrBr having $I_{calc} > 1$ (on a scale of 0-10) which may overlap lines of $ZrBr_x$.

Table A-3. Guinier powder pattern of $ZrBr_{1.8(2)}$[a]

h k l	I_{obs}	d_{calc}	d_{obs}	h k l	I_{obs}	d_{calc}	d_{obs}
0 0 1		13.73		1 0 8	1	1.4958	1.4959
0 0 2	4	6.86	6.88	2 0 2	1	1.4902	1.4898
0 0 3		4.575		1 1 5		1.4833	
0 0 4	1	3.432	3.434	2 0 3	4	1.4482	1.4481
1 0 0	5	3.053	3.055	1 1 6	2	1.3964	1.3964
1 0 1		2.980		2 0 4		1.3949	
1 0 2	1*	2.790	2.790	0 0 10		1.3726	
0 0 5		2.745		1 0 9		1.3644	
1 0 3	8	2.540	2.541	2 0 5	1*	1.3342	1.3344
0 0 6	1	2.288	2.288	1 1 7		1.3110	
1 0 4	1	2.281	2.280	2 0 6	1	1.2699	1.2699
1 0 5	3	2.041	2.041	1 0 10		1.2519	
0 0 7		1.9609		0 0 11		1.2478	
1 0 6	1	1.8308	1.8307	1 1 8	2	1.2295	1.2295
1 1 0	10	1.7628	1.7633	2 0 7		1.2046	
1 1 1		1.7485		1 0 11		1.1551	
0 0 8	1	1.7157	1.7159	2 1 0	2	1.1541	1.1541
1 1 2	2	1.7074	1.7074	1 1 9		1.1534	
1 0 7		1.6499		2 1 1		1.1500	
1 1 3		1.6450		0 0 12	1*	1.1438	1.1436
1 1 4	1	1.5680	1.5676	2 0 8	1	1.1405	1.1405
2 0 0	3	1.5267	1.5267	2 1 2	1	1.1381	1.1380
0 0 9		1.5251		2 1 3	5	1.1190	1.1192
2 0 1		1.5173		2 1 4		1.0939	

[a]Based on a primitive hexagonal cell with $\underline{a}$=3.5257(2) and $\underline{c}$=13.726(2) computed by the CDR program from all 23 non-ZrBr lines in a powder pattern of $ZrBr_{1.42}$(Table 4, text). The three indicated (*) reflections are of uncertain intensity because of overlap with ZrBr lines.

Table A-4. Indexed Guinier powder pattern of $ZrCl_{1.6}$[a]

h	k	l	θ_{obs}	θ_{calc}	d_{calc}	I_{obs}
0	0	3	6.83	6.84	6.463	10
0	0	6	13.79	13.79	3.232	1
1	0	0	15.25	15.24	2.930	1
1	0	1	15.42	15.42	2.897	6
1	0	2	15.94	15.94	2.804	6
1	0	4	17.89	17.89	2.507	8
0	0	8	18.55	18.53	2.424	2
1	0	5	19.23	19.24	2.338	8
0	0	9	20.95	20.95	2.154	5
1	0	7	22.50	22.50	2.013	5
1	0	8	24.36	22.36	1.868	4
1	0	9	26.32	26.35	1.736	4
1	1	0	27.09	27.09	1.6915	8
1	1	3	28.07	28.08	1.6364	5
0	0	12	28.47	28.47	1.6158	4
1	0	11	30.66	30.66	1.5104	2
1	1	6	30.94	30.93	1.4986	2
2	0	0*	31.70	31.73	1.4649	1
2	0	1	31.83	31.83	1.4607	3
2	0	2	32.13	32.13	1.4484	3
2	0	4	33.33	33.32	1.4023	4
2	0	5	34.21	34.20	1.3704	4
1	1	9	35.39	35.38	1.3304	7
2	0	7	36.51	36.50	1.2950	3
2	0	8	37.91	37.91	1.2537	2
1	0	14	37.95	37.97	1.2521	2
1	1	12*	41.24	41.24	1.1686	7
2	0	10*	41.24	41.24	1.1686	
2	0	11	43.14	43.14	1.1266	2
1	0	16	43.47	43.46	1.1199	3
2	1	1	44.17	44.17	1.1055	3
2	1	2	44.44	44.44	1.1002	3

[a]All reflections except those indicated (*) were used for a final least squares lattice refinement to give hexagonal cell parameters of a=3.3829(2) and c=19.390(1).

[b]Products prepared at temperatures above 600° show an increasing tendency toward broad bands in these regions.

Table A-5. Calculated Guinier powder pattern of Zr_6Cl_{15}[a]

d_{calc}	I_{calc}	N[b]	h	k	l[c]	d_{calc}	I_{calc}	N	h	k	l
7.47	1000	1	2	2	0	1.8263	73	4	11	3	2
5.650	61	1	3	2	1	1.7996	35	2	11	4	1
4.315	35	1	4	2	2	1.7496	55	4	9	8	1
3.737	41	1	4	4	0	1.7262	47	3	10	7	1
3.430	49	2	5	3	2	1.7036	38	2	12	3	1
3.343	73	1	6	2	0	1.6409	38	3	9	9	2
3.262	91	1	5	4	1	1.5178	52	4	9	8	7
2.877	176	3	5	5	2	1.5024	38	4	13	5	2
2.527	113	1	6	5	3	1.3061	39	2	10	9	9
2.492	38	2	8	2	2	1.2962	31	5	13	9	4
2.458	212	3	7	4	3	1.2866	34	4	11	10	7
2.394	31	1	7	5	2	1.2165	31	3	14	9	5
2.280	110	3	7	6	1	1.1236	43	3	13	11	8
2.228	102	3	7	5	4	1.0597	54	5	17	10	3
2.136	70	2	8	5	3	1.0518	41	3	16	12	2
2.093	67	2	7	7	2	1.0441	54	4	20	3	1
2.073	40	2	10	2	0	1.0390	43	5	17	10	5
1.9462	30	3	10	3	3	1.0243	85	6	20	5	1

[a]Lines are omitted from this listing if the combined intensity for all reflections at a given d value is less than 30 relative to I_{calc}=1000 for (2 2 0).

[b]N=the number of reflections contributing to I_{calc} at a given d.

[c]The representative hkl listed when N > 1 is the one with greatest I_{calc}.

Table A-6. Powder diffraction data for ZrBr[a]

h k l	d_{calc}[b]	I_{obs} (Guin.)	I_{obs} (D.S.)	h k l	d_{calc}	I_{obs} (Guin.)	I_{obs} (D.S.)
0 0 3	9.357	14	20	1 0 17	1.4503	8	20
0 0 6	4.678	8	20	2 0 7	1.4188	11	5
0 0 9	3.119	0	0	1 1 12	1.4021	21	25
1 0 1	3.016	15	5	2 0 8	1.3924	0	0
1 0 2	2.965	17	25	0 0 21	1.3367	0	20
1 0 4	2.785	9	5	2 0 10	1.3345	13	
1 0 5	2.669	100	100	1 0 19	1.3283	0	0
1 0 7	2.419	19	30	2 0 11	1.3039	1	0
0 0 12	2.339	8	35	1 1 15	1.2788	17	25
1 0 8	2.295	0	0	1 0 20	1.2738	1	0
1 0 10	2.060	30	40	2 0 13	1.2412	0	0
1 0 11	1.9529	3	5	2 0 14	1.2097	0	0
0 0 15	1.8714	5	28	1 0 22	1.1762	4	20
1 0 13	1.7592	3	5	0 0 24	1.1696	0	0
1 1 0	1.7515	50	40	1 1 18	1.1647	4	10
1 1 3	1.7216	8	5	2 0 16	1.1475	1	0
1 0 14	1.6727	0	0	2 1 1	1.1457	1	0
1 1 6	1.6404	11	5	2 1 2	1.1429	5	5
0 0 18	1.5595	1	10	1 0 23	1.1323	2	0
1 1 9	1.5272	0	0	2 1 4	1.1317	0	0
1 0 16	1.5188	5	5	2 1 5	1.1235	29	20
2 0 1	1.5147	0		2 0 17	1.1171	2	5
2 0 2	1.5081	11	5	2 1 7	1.1025	6	5
2 0 4	1.4826	0	0	2 1 8	1.0899	0	0
2 0 5	1.4644	38	25				

[a]Guinier intensities are from a microdensitometer film scan while Debye-Scherrer intensities were visually estimated.

[b]All observed reflections are within ±0.02° of θ_{calc} for lattice parameters of $\underline{a}$=3.5031(3) and $\underline{c}$=28.071(3).

Table A-7. Hexagonal lattice constants for α-Zr, some indexed zirconium halides, and HfCl

Phase Composition	N[a]	a (Å)	c (Å)	Preparative Method
α-Zr	11	3.2328(4)	5.1505(9)	$ZrCl \xrightarrow{1054^\circ} Zr^\circ + ZrCl_4(g)$
ZrCl	9	3.4212(3)	26.693(3)	Equilibration with Zr (975°)
	10	3.4233(5)	26.692(4)	Equilibration with Zr (1054°)
ZrBr	23	3.5031(3)	28.071(3)	Stoichiometric prep (825°)
$ZrBr_{1-x}O_x$	22	3.5646(2)	28.479(5)	ZrBr + xs ZrO_2 (850°,6d)
HfCl[b]	24	3.3697(3)	26.582(6)	$HfCl_{1.3}$ + xs Hf (650°,6d)
$ZrCl_{1.6}$	28	3.3830(2)	19.390(1)	$ZrCl_3$ + xs ZrCl (600°,35d)
$ZrBr_{1.8}$	21	3.5257(2)	13.726(2)	ZrBr + xs $ZrBr_3$ (600°,28d)

[a]The number of unambiguously assigned reflections input to the CDR program.

[b]Based on a Debye-Scherrer film read and corrected for shrinkage by A.W. Struss and reported in an earlier publication (22).

BIBLIOGRAPHY

1. A. Simon, Chemie in unserer Zeit, 10(1), 1 (1976).

2. J. E. Fergusson in "Preparative Inorganic Reactions," Vol. 5, W. L. Jolly, Ed., Wiley, New York, 1971, p. 93.

3. H. Schäfer, Arbeitsgem. Forsch. Landes Nordrhein-Westfalen, 192, 7 (1969).

4. F. A. Cotton, Accounts Chem. Res., 2, 240 (1969).

5. H. Schäfer and H. G. Schnering, Angew. Chem., 76, 833 (1964).

6. J. Lewis and R. S. Nyholm, Sci. Progr., 52, 557 (1964).

7. B. R. Penfold in "Perspectives in Structural Chemistry," Vol. II, J. D. Dunitz and J. A. Ibers, Ed., Wiley, New York, 1968, p. 71.

8. M. C. Baird, Progr. Inorg. Chem., 9, 1 (1968).

9. L. F. Dahl and D. L. Wampler, Acta Crystallogr., 15, 903 (1962).

10. D. G. Adolphson, Ph.D. Thesis, Iowa State University, Ames, Iowa (1975).

11. D. G. Adolphson and J. D. Corbett, Inorg. Chem., in press (1976).

12. H. G. von Schnering, H. Wöhrle, and H. Schäfer, Naturwissenschaften, 48, 159 (1961).

13. A. Simon, H. G. Schnering, H. Wöhrle, and H. Schäfer, Z. Anorg. Allg. Chem., 339, 155 (1965).

14. D. Bauer and H. G. von Schnering, Z. Anorg. Allg. Chem., 361, 259 (1968).

15. L. F. Dahl, T. Chiang, P. W. Seabaugh, and E. M. Larsen, Inorg. Chem., 3(9), 1236 (1964).

16. J. A. Watts, Inorg. Chem., 5(2), 281 (1966).

17. F. A. Cotton and J. T. Mague, Inorg. Chem., 3(10), 1402 (1964).

18. M. J. Bennett, F. A. Cotton, and B. M. Foxman, Inorg. Chem., 7(8), 1563 (1968).

19. O. Ruff and R. Wallstein, Z. Anorg. Chem., 128, 96 (1923).

20. I. E. Newnham and J. A. Watts, J. Amer. Chem. Soc., 82, 2133 (1960).

21. G. W. Watt and W. A. Baker, Jr., J. Inorg. Nucl. Chem., 22, 49 (1961).

22. A. W. Struss and J. D. Corbett, Inorg. Chem., 9(6), 1373 (1970).

23. D. B. Copley and R. A. J. Shelton, J. Less-Common Metals, 20, 359 (1970).

24. S. I. Troyanov, V. I. Tsirel'nikov, and L. N. Komissarova, Izv. Vyssh. Ucheb. Zaved., Khim. Khim. Tekhnol., 12, 851 (1969). (Chem. Abstr., 72, 18008e (1970)).

25. S. I. Troyanov, G. S. Marek, and V. I. Tsirel'nikov, Zh. Fiz. Khim., 48, 2671 (1974). (Chem. Abstr., 82, 50797d (1975)).

26. E. M. Larsen and J. J. Leddy, J. Amer. Chem. Soc., 78, 5983 (1956).

27. A. S. Normanton and R. A. J. Shelton, J. Less-Common Metals, 32, 111 (1973).

28. S. I. Troyanov and V. I. Tsirel'nikov, Zh. Fiz. Khim., 48, 1988 (1974).

29. F. R. Sale and R. A. J. Shelton, J. Less-Common Metals, 9, 64 (1965).

30. A. K. Baev and R. A. J. Shelton, Zh. Fiz. Khim., 47, 2382 (1973).

31. A. W. Struss and J. D. Corbett, Inorg. Chem., 8(2), 227 (1969).

32. E. M. Larsen, F. Gil-Arnao, J. W. Moyer, and M. J. Camp, Chem. Commun., 281 (1970).

33. E. M. Larsen, J. W. Moyer, F. Gil-Arnao, and M. J. Camp, Inorg. Chem., 13(3), 574 (1974).

34. J. Kleppinger, J. C. Calabrese, and E. M. Larsen, Inorg. Chem., 14(12), 3128 (1975).

35. J. Kleppinger, J. C. Calabrese, and E. M. Larsen, 170th Natl. Mtg. Amer. Chem. Soc., Aug. 25-29, 1975, Inorg. Chem. Div., Abstr. 178.

36. B. Swaroop and S. N. Flengas, Can. J. Chem., 43, 2115 (1965).

37. F. R. Sale and R. A. J. Shelton, J. Less-Common Metals, 9, 60 (1965).

38. A. G. Turnbull and J. A. Watts, Aust. J. Chem., 16(6), 947 (1963).

39. K. Uchimura and K. Funaki, Denki Kagaku-shi, 33, 163 (1965); translation LA-TR-67-62 available from CFSTI, U. S. Department of Commerce, Springfield, Va.

40. H. L. Schläfer and H. Skoludek, Z. Elektrochem., 66(4), 367 (1962).

41. V. I. Tsirel'nikov, J. Less-Common Metals, 19, 287 (1969).

42. E. H. Hall and J. M. Blocher, Jr., J. Phys. Chem., 63, 1525 (1959).

43. B. G. Newland and R. A. J. Shelton, J. Less-Common Metals, 20, 245 (1970).

44. F. K. McTaggart and A. G. Turnbull, Aust. J. Chem., 17(7), 727 (1964).

45. M. Fukutomi, Ames Laboratory, USERDA, Iowa State University, Ames, Iowa, personal communication, 1975.

46. R. S. Dean, U. S. Patent 2,941,931, June 21, 1960.

47. S. I. Troyanov and V. I. Tsirel'nikov, Russ. J. Inorg. Chem., 15(12), 1762 (1970).

48. S. I. Troyanov, Vestn. Mosk. Univ., Khim., 28, 369 (1973).

49. K. Yvon, W. Jeitschko, and E. Parthé, Laboratory for Research on the Structure of Matter, University of Pennsylvania, Philadelphia, 1969.

50. R. A. Jacobson, "An Algorithm for Automatic Indexing and Bravais Lattice Selection: The Programs BLIND and ALICE," USAEC Report IS-3469, 1974.

51. "International Tables of X-ray Crystallography," Vol. I, Kynoch Press, Birmingham, England, 1952.

52. E. Drent, C. A. Emeis, and A. G. T. G. Kortbeek, Solid State Commun., 16, 1351 (1975).

53. A. R. Janus, Ph.D. Thesis, Syracuse University, Syracuse, New York (1964).

54. F. Kadijk, R. Huisman, and F. Jellinek, Rec. Trav. Chim., 83, 768 (1964).

55. R. Huisman, F. Kadijk, and F. Jellinek, J. Less-Common Metals, 12, 423 (1967).

56. K. Lascelles and R. A. J. Shelton, J. Less-Common Metals, 25, 49 (1971).

57. F. Jellinek, G. Brauer, and H. Müller, Nature (London), 185, 376 (1960).

58. K. Poeppelmeier, Ames Laboratory, USERDA, Iowa State University, Ames, Iowa, personal communication, 1976.

59. A. S. Izmailovich, S. I. Troyanov, and V. I. Tsirel'nikov, Zh. Neorg. Khim., 19, 2922 (1974).

60. A. Simon, H. Mattausch, and N. Holzer, Angew. Chem., in press (1976).

61. F. R. Gamble, J. H. Osiecki, M. Cais, R. Pisharody, F. J. DiSalvo, and T. H. Geballe, Science, 174, 493 (1971).

62. A. Struss, Ames Laboratory, USERDA, Iowa State University, Ames, Iowa, personal communication, 1976.

63. V. I. Nefedov, Y. V. Salyn', A. A. Chertkov, and L. N. Padurets, Zh. Neorg. Khim., 19, 1443 (1974).

64. B. Krebs, Z. Anorg. Allg. Chem., 368, 263 (1970).

65. P. Main, M. M. Woolfson, and F. Germain, "MULTAN, A Computer Program for the Automatic Solution of Crystal Structures," University of York Printing Unit, York, U. K., 1971.

66. W. R. Busing, K. O. Martin, and H. A. Levy, USAEC Report ORNL-TM-305, Oak Ridge National Laboratory, Oak Ridge, Tennessee, 1962.

67. C. R. Hubbard, C. O. Quicksall, and R. A. Jacobson, USAEC Report IS-2625, Ames Laboratory, USAEC, Iowa State University, Ames, Iowa, 1971.

68. J. Springer, Department of Chemistry, Iowa State University, Ames, Iowa, personal communication, 1976.

69. R. E. McCarley, Ames Laboratory, USERDA, Iowa State University, Ames, Iowa, personal communication, 1976.

70. W. R. Busing, K. O. Martin, and H. A. Levy, USAEC Report ORNL-TM-306, Oak Ridge National Laboratory, Oak Ridge, Tennessee, 1964.

71. P. J. Kuhn and R. E. McCarley, Inorg. Chem., 4(10), 1482 (1965).

72. H. Schäfer and D. Giegling, Z. Anorg. Allg. Chem., 420, 1 (1976).

73. H. Schäfer, H. G. Schnering, K. J. Niehues, and H. G. Niedervahrenholz, J. Less-Common Metals, 9, 95 (1965).

74. D. Bauer and H. Schäfer, J. Less-Common Metals, 14, 476 (1968).

75. C. K. Johnson, USAEC Report ORNL-3794, Revised, Oak Ridge National Laboratory, Oak Ridge, Tennessee, 1965.

76. F. A. Cotton and T. E. Haas, Inorg. Chem., 3(1), 10 (1964).

77. J. C. Wood, B. A. Surette, I. M. London, and J. Baird, J. Nucl. Mater., 57, 155 (1975).

78. H. Schäfer, Z. Anorg. Allg. Chem., 403, 116 (1974).

79. D. Bauer, H. G. Schnering, and H. Schäfer, J. Less-Common Metals, 8, 388 (1965).

80. A. Simon, H. G. von Schnering, and H. Schäfer, Z. Anorg. Allg. Chem., 355, 295 (1967).

81. L. R. Bateman, J. F. Blount, and L. F. Dahl, J. Amer. Chem. Soc., 88, 1082 (1966).

82. A. Simon, H. G. von Schnering, and H. Schäfer, Z. Anorg. Allg. Chem., 361, 235 (1968).

ACKNOWLEDGMENTS

The author especially wishes to express his appreciation to Professor John D. Corbett for his helpful suggestions and creative feedback during the course of this work. He also wishes to thank Professor H. F. Franzen and Dr. Mirtha Umaña for acquiring the XPS data presented here, and Professor R. A. Jacobson for providing the diffractometer and programs for collection of single crystal data. The author is grateful to Bob Daake for taking vacation time to write the Guinier Film Measuring Program which has saved tedious hours of repetitive calculations, and he cannot overlook the patience of his typist wife who invested many tiring days in preparing this typewritten manuscript.

Since joining Physical and Inorganic Chemistry Group IX of the Ames Laboratory, the author has enjoyed both serious and humorous discussions with other Group members, and is particularly grateful to Art Struss and A. V. Hariharan for their constructive criticisms and friendly encouragement during the course of this research.